Four-field excitation of multiphoton NMR resonances in spin $I=\frac{1}{2}$

Eric M. Krauss and Shimon Vega
Department of Isotope Research, The Weizmann Institute of Science, 76100 Rehovot, Israel
(Received 18 November 1985)

The use of four pulsed rf fields for the excitation of multiphoton resonances in a two-level system is investigated. A general theoretical description of the experiment is provided based on the Floquet formalism and application of basic conservation laws to the overall transition process. The predictions of the theory are compared with computer simulations of the time evolution of the magnetization according to the exact time-dependent Hamiltonian. It is shown that N-photon resonances occur when the fields are applied at frequencies $\pm k\omega$ and $\pm l\omega$ from the Larmor frequency, where k and l are positive integers having no common factors and where $0\leq k<l$, $k+l=N$. For any resonance k photons are taken from the outer field pair and l are taken from the inner field pair. A total of $2[(l+k)!]/(k!l!)$ mutually interfering transition pathways exist for the overall process and the resultant magnitude of the effective N-photon field is very sensitive to the relative initial phases of the rf fields. The spiral motion observed for multiphoton resonances induced by double-frequency irradiation is absent here when the field intensities are symmetrical. In addition, the fraction of total applied rf intensity available for multiphoton pumping is considerably greater than for two fields. Phase cycling to enhance detection of multiphoton effects and multiphoton spin locking are considered.

I. INTRODUCTION

The nonlinear response of a two-level system to two simultaneously applied irradiation fields has been the subject of intensive study.[1-18] When the oscillating fields are the components of a single strong linearly polarized field oscillating in the plane normal to the quantization axis of the system, it has been demonstrated theoretically[1-9] and experimentally[7-11] that subsidiary resonances appear when the ratio of the applied frequency to the Larmor frequency, Ω/Ω_0, is approximately $1/N$, $N=3,5,7,\ldots$. Formulations of the problem utilizing Floquet's theorem[4-6] and the second quantization[7-9] have established resonance conditions and afforded a description of the subsidiary resonance as a process in which a total of N photons are absorbed from and emitted to the two circularly polarized field components during transition between atomic states. By application of perturbation theory, a time-independent effective Hamiltonian determining the approximate time evolution of the system near resonance could be derived, the off-diagonal element of which was proportional to ω_1^N/Ω^{N-1}, where ω_1 is the oscillating field intensity. Multiphoton resonances predicted by the theory have been detected by microwave spectroscopy,[10] molecular beam methods,[8] and optical pumping.[7,9,11]

While NMR can, in principle, directly detect multiphoton resonances in a system of noninteracting spins-$\frac{1}{2}$ under linearly polarized rf irradiation, its inherent lack of sensitivity precludes this at achievable rf field strengths. Consequently, the influence of the counterrotating rf component in NMR is conventionally disregarded.[12] These effects become experimentally accessible with double-frequency irradiation near the Larmor frequency.[13-18] Two linearly polarized rf fields applied at frequencies Ω_1 and Ω_2 will, in a frame rotating at frequency $\Omega_{av}=\frac{1}{2}(\Omega_1+\Omega_2)$, assume the roles played by the components of the single linearly polarized field in the laboratory frame, and $\Delta m=1$ transitions involving the absorption and emission of several photons are possible.[18] The resonance condition here is $|(\Omega_1-\Omega_{av})/(\Omega_0-\Omega_{av})|\approx 1/N$, N odd. The N-photon effective field varies inversely as $(\Omega_1-\Omega_{av})^{N-1}$, rather than Ω^{N-1} as above, so that considerably lower rf field intensities are necessary. Anderson[13] directly observed an $N=3$ transition in water by irradiating with two rf fields, while Franz and Slichter[14] observed up to three photon transitions in rotary saturation experiments on solid CaF_2. In a series of studies of the ^1H NMR response of chloroform to double-frequency irradiation, Bucci, Santucci, and coworkers[15-17] detected all possible multiphoton resonances up to $N=27$ with Ω_1 fixed and Ω_2 variable. These early NMR experiments were all of the continuous wave (cw) type, and coherent effects during multiphoton excitation were not observed.

Zur *et al.*[18] extended these studies to the pulsed NMR regime by using two simultaneous pulsed rf fields to invert the ^{31}P magnetization of phosphoric acid by a three-photon pathway. An inversion time t_π of less than 2 ms was obtained with rf field intensities of 10 kHz. A theoretical treatment based on single-mode Floquet theory was presented and an expression for the three-photon effective field obtained. The rf fields were phase synchronized, and the dependence of the phase of the coherence created by double-frequency irradiation on the initial rf field phases was found to be consistent with a transition process involving two inner-field (closest in frequency to Ω_0) absorptions and one outer-field emission. The magnitude of the effective field, measured directly as π/t_π, was proportional to the outer rf field intensity and to the square of the inner rf field intensity, and was independent of the initial phases, in agreement with the theory.

A characteristic spiral motion executed by the magnetization in the Larmor frame during resonant double-frequency irradiation was also observed by Zur *et al.* This motion originates in a Bloch-Siegert-like shift, relative to the Larmor frame, of the rotating frame in which the magnetization undergoes simple processional motion under a time-independent effective Hamiltonian. In the cw spectra this is manifested as rf field strength-dependent shifts of the multiphoton resonance positions.[16] While generally a negligible effect in pulsed single-quantum NMR spectroscopy, spiral motion substantially complicates the coherent detection of multiphoton processes because the spiraling frequency is not small in comparison to the magnitude in frequency units of the effective multiphoton field. For the three-photon process cited above, many cycles of the spiral motion were completed during time t_π. This rapid (in comparison to t_π^{-1}) motion could not be suppressed and more elaborate pulse schemes were devised[18] for determining the magnitude and phase of the transverse magnetization after multiphoton excitation.

Double-frequency irradiation has also been used to create double-quantum coherence in a spin $I=1$ system in the solid state.[19] When the fields were symmetrically placed about Ω_0 and the field intensities set equal, the magnetization was found to execute a simple nutation about I_x^{1-3} in the Larmor frame without spiraling. The rf was generated by amplitude modulation of the carrier wave. In order for there to be no spiraling, it was necessary that both the rf field positions and intensities be symmetric about Ω_0, a form of irradiation which cannot induce transitions in a two-level system.[18] However, the response of a spin-$\frac{1}{2}$ system to more than one pair of rf fields has not been explored.

The present study treats theoretically the response of a spin-$\frac{1}{2}$ system to up to four simultaneously applied rf fields. The fields are assumed to be symmetrically disposed about a central frequency Ω_0, with arbitrary intensities and phases (Fig. 1). The most general configuration of this type would be prepared by low-frequency amplitude—and phase—modulation of an rf carrier at frequency Ω, with selective attenuation to fix the relative intensities of each frequency component. In Sec. II, the Floquet formalism for periodic time-dependent Hamiltonians and perturbation theory are employed to obtain an approximate time-independent Hamiltonian for the problem, from which conditions for resonance without spiraling can directly be established. The existence of these resonances depends on the connectivity of the Floquet states and the fulfillment of basic conservation laws for the overall transition process. Once the resonance conditions are defined, expressions for the off-diagonal element of the effective Hamiltonian are derived. Section III presents a series of accurate computer simulations of the motion of the magnetization vector calculated according to the exact time-dependent Hamiltonian for field configurations predicted by the theory to induce multiphoton resonances. It is found that the response to four fields differs qualitatively from that to two fields, most notably with regard to the existence of more than one resonance of given order N, the presence of many mutually interfering transition pathways for any resonance, and the total suppression of spiraling under readily achieved conditions.

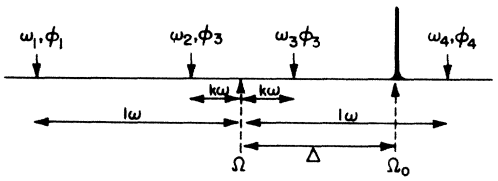

FIG. 1. General irradiation scheme: four rf fields of arbitrary intensity and phase are applied at frequencies $\pm k\omega, \pm l\omega$ from a central frequency Ω, where k and l are positive integers having no common factors and $0 \leq k < l$. The offset from the Larmor frequency Ω_0 is $\Delta = \Omega_0 - \Omega$.

II. THEORY

A. The Hamiltonian

The laboratory-frame Hamiltonian for a spin $I=\frac{1}{2}$ of Larmor frequency Ω_0 irradiated simultaneously by four rf fields symmetrically placed about a frequency Ω as shown in Fig. 1 is

$$\mathcal{H}_L(t) = -\Omega_0 I_z - 2I_x\{\omega_1\cos[(\Omega - l\omega)t - \phi_1] + \omega_2\cos[(\Omega - k\omega)t - \phi_2] + \omega_3\cos[(\Omega + k\omega)t - \phi_3] + \omega_4\cos[(\Omega + l\omega)t - \phi_4]\}\ , \tag{1}$$

where $2\omega_j$ and ϕ_j are the amplitude and initial phase of field j, $\omega > 0$, and k and l are positive integers having no common factors besides one, defined such that $0 \leq k < l$. In a frame rotating at frequency Ω about the static field direction,

$$\mathcal{H}(t) = -\Delta I_z - I_x[\omega_1\cos(l\omega t + \phi_1) + \omega_2\cos(k\omega t + \phi_2) + \omega_3\cos(k\omega t - \phi_3) + \omega_4\cos(l\omega t - \phi_4)] - I_y[\omega_1\sin(l\omega t + \phi_1) + \omega_2\sin(k\omega t + \phi_2) - \omega_3\sin(k\omega t - \phi_3) - \omega_4\sin(l\omega t - \phi_4)]\ , \tag{2}$$

with $\Delta \equiv \Omega_0 - \Omega$. The counterrotating components of the fields are neglected in Eq. (2).

The solution of the equation of motion for the spin density matrix, neglecting relaxation effects, can formally be written

$$\rho(t)=U(t)\rho(0)U^{-1}(t)\ , \tag{3}$$

where $U(t)$ must be determined from the time-dependent Hamiltonian of Eq. (2). Equation (3) can be evaluated numerically by division of the evolution time t into many subintervals over which the Hamiltonian is nearly constant.[19] This procedure is utilized in Sec. III to study the exact time evolution of the magnetization when multiphoton resonance conditions are satisfied.

B. The effective Hamiltonian

In order to establish conditions for resonance, an approximate expression for the evolution operator $U(t)$ will be obtained based on the Floquet formalism for periodic time-dependent Hamiltonians. A thorough description of the methods has appeared[18] and only expressions which are essential or require modification will be reproduced here. If $\mathscr{H}(t)$ is periodic with period $2\pi/\omega$, the elements of $U(t)$ are given by

$$U_{\gamma\eta}(t)=\sum_{n=-\infty}^{\infty}\langle\gamma,n\,|\,e^{-i\mathscr{H}_F t}\,|\,\eta,0\rangle e^{in\omega t}\ . \tag{4}$$

The Floquet Hamiltonian $\mathscr{H}_F$ is an infinite time-independent matrix with elements

$$\langle\gamma,m+n\,|\,\mathscr{H}_F\,|\,\eta,m\rangle=\mathscr{H}^{(n)}_{\gamma\eta}+m\omega\delta_{\gamma\eta}\delta_{n0}\ , \tag{5}$$

where

$$\mathscr{H}_{\gamma\eta}(t)=\sum_{n=-\infty}^{\infty}\mathscr{H}^{(n)}_{\gamma\eta}e^{in\omega t}\ . \tag{6}$$

The Floquet states $|\gamma n\rangle$ are equivalent to dressed spin states labeled by the eigenstates of the Zeeman Hamiltonian, γ, and the reduced photon number n. For the Hamiltonian of Eq. (2), the nonzero elements of $\mathscr{H}_F$ are

$$\begin{aligned}
&\langle\alpha,m\,|\,\mathscr{H}_F\,|\,\alpha,m\rangle=-\frac{\Delta}{2}+m\omega,\\
&\langle\beta,m\,|\,\mathscr{H}_F\,|\,\beta,m\rangle=\frac{\Delta}{2}+m\omega\ ,\\
&\langle\beta,m+l\,|\,\mathscr{H}_F\,|\,\alpha,m\rangle=\langle\alpha,m-l\,|\,\mathscr{H}_F\,|\,\beta,m\rangle^*=X_1\ ,\\
&\langle\beta,m+k\,|\,\mathscr{H}_F\,|\,\alpha,m\rangle=\langle\alpha,m-k\,|\,\mathscr{H}_F\,|\,\beta,m\rangle^*=X_2\ ,\\
&\langle\beta,m-k\,|\,\mathscr{H}_F\,|\,\alpha,m\rangle=\langle\alpha,m+k\,|\,\mathscr{H}_F\,|\,\beta,m\rangle^*=X_3\ ,\\
&\langle\beta,m-l\,|\,\mathscr{H}_F\,|\,\alpha,m\rangle=\langle\alpha,m+l\,|\,\mathscr{H}_F\,|\,\beta,m\rangle^*=X_4\ ,
\end{aligned} \tag{7}$$

where $|\alpha\rangle$ and $|\beta\rangle$ are eigenstates of I_z with eigenvalues $\frac{1}{2}$ and $-\frac{1}{2}$, respectively, m is any integer, and

$$X_j=-\tfrac{1}{2}\omega_j e^{i\phi_j},\quad j=1,2,3,4\ . \tag{8}$$

In setting up $\mathscr{H}_F$ we have, for reasons of convenience, employed a lumped photon index and the notation of single-mode Floquet theory, rather than invoke two or four separate photon numbers. Since k and l are relatively prime, there will be no ambiguity as to which rf field is involved in any step of a multistep transition process. Furthermore, in the limit of large photon numbers the matrix elements between dressed states will depend only on the differences between, not the absolute values of, the photon numbers of the states.[5,16]

Considerable simplification of Eq. (4) is possible if the off-diagonal elements of $\mathscr{H}_F$ are smaller than the differences between diagonal elements ($\omega_j \ll \omega$), as will generally be assumed in this study. The diagonal elements of $\mathscr{H}_F$ depend on Δ and ω (as well as the secular parts of interaction Hamiltonians, if present). As the external parameters are varied, resonance between Floquet states $|\gamma,n\rangle$ and $|\eta,0\rangle$ will occur if for some set of parameter values collectively denoted by P there exist n, γ, and η such that (i) $\langle\gamma,m+n\,|\,\mathscr{H}_F(P)\,|\,\gamma,m+n\rangle=\langle\eta,m\,|\,\mathscr{H}_F(P)\,|\,\eta,m\rangle$, $m=0,\pm1,\pm2,\ldots$ and (ii) the quantity

$$\begin{aligned}
-\tfrac{1}{2}\omega^{\gamma\eta}_{\mathfrak{P}}=&\sum_{\substack{(\gamma',i)\\[\neq(\gamma,n),(\eta,0)]}}\frac{\langle\gamma,n\,|\,\mathscr{H}_F(P)\,|\,\gamma',i\rangle\langle\gamma',i\,|\,\mathscr{H}_F(P)\,|\,\eta,0\rangle}{E^n_{\gamma\eta}-E_{\gamma' i}}\\
&+\sum_{\substack{(\gamma',i),(\eta',j)\\[\neq(\gamma,n),(\eta,0)]}}\frac{\langle\gamma,n\,|\,\mathscr{H}_F(P)\,|\,\gamma',i\rangle\langle\gamma',i\,|\,\mathscr{H}_F(P)\,|\,\eta',j\rangle\langle\eta',j\,|\,\mathscr{H}_F(P)\,|\,\eta,0\rangle}{(E^n_{\gamma\eta}-E_{\gamma' i})(E^n_{\gamma\eta}-E_{\eta' j})}+\cdots
\end{aligned} \tag{9}$$

is nonzero; here, $E_{\gamma j}=E_{\gamma j}(P)=\langle\gamma,j\,|\,\mathscr{H}_F(P)\,|\,\gamma,j\rangle$ and $E^n_{\gamma\eta}=(E_{\gamma n}+E_{\eta 0})/2$. When the two conditions are satisfied for weak rf fields the time dependence of $\rho(t)$ is essentially confined to coherence between levels γ and η, and time-independent perturbation theory can be applied to $\mathscr{H}_F(P)$ to obtain

$$U^{\gamma-\eta}(t)=e^{in\omega t I_z^{\gamma-\eta}}e^{-i\mathscr{H}^{\gamma-\eta}_{\mathfrak{P}}t}\ , \tag{10}$$

$U^{\gamma-\eta}(t)$ is the part of $U(t)$ active on the resonant levels and is identical to $U(t)$ for spin $I=\frac{1}{2}$. The effective Hamiltonian is a 2×2 time-independent matrix defined in terms of fictitious spin-$\frac{1}{2}$ operators in the $|\gamma,n\rangle,|\eta,0\rangle$ manifold by

$$\mathscr{H}^{\gamma-\eta}_{\mathfrak{P}}=-\mathrm{Re}(\omega^{\gamma\eta}_{\mathfrak{P}})I_x^{\gamma-\eta}+\mathrm{Im}(\omega^{\gamma\eta}_{\mathfrak{P}})I_y^{\gamma-\eta}-\delta^{\gamma\eta}_{\mathfrak{P}}I_z^{\gamma-\eta}\ . \tag{11}$$

The offset parameter is

$$\delta^{\gamma\eta}_{\mathfrak{P}}=E_{\eta 0}-E_{\gamma n}+\delta^{\eta}_0-\delta^{\gamma}_n\ , \tag{12}$$

where the perturbation correction δ_n^γ to the energy of Floquet state $|\gamma,n\rangle$ due to interaction with nonresonant levels is

$$\delta_n^\gamma = \sum_{\substack{(\gamma',i) \\ [\neq(\gamma,n),(\eta,0)]}} \frac{\langle\gamma,n|\mathscr{H}_F(P)|\gamma',i\rangle\langle\gamma',i|\mathscr{H}_F(P)|\gamma,n\rangle}{E_{\gamma\eta}^n - E_{\gamma',i}} + \sum_{\substack{(\gamma',i),(\eta',j) \\ [\neq(\gamma,n),(\eta,0)]}} \frac{\langle\gamma,n|\mathscr{H}_F(P)|\gamma',i\rangle\langle\gamma',i|\mathscr{H}_F(P)|\eta',j\rangle\langle\eta',j|\mathscr{H}_F(P)|\gamma,n\rangle}{(E_{\gamma\eta}^n - E_{\gamma'i})(E_{\gamma\eta}^n - E_{\eta'j})} + \cdots . \tag{13}$$

Equation (10) gives an approximate evolution operator in the frame in which $\mathscr{H}(t)$ is determined, rotating at angular frequency Ω. Transformation to a frame rotating at angular frequency $\Omega+n\omega$ gives the familiar expression

$$U^{\gamma-\eta}(t)' = e^{-i\mathscr{H}_P^{\gamma-\eta}t} . \tag{14}$$

The system evolves according to a time-independent effective Hamiltonian in the $\Omega+n\omega$ frame. In any other rotating frame, the magnetization executes spiral motion.[18]

A remark is in order concerning the relation of the present approach to average Hamiltonian theory (AHT). It can be shown[20] that if the series in Eq. (9) is truncated after the terms containing some number N' factors, the resulting $-\frac{1}{2}\omega_P^{\gamma\eta}$ is equivalent to the (γ,η) element of $\hat{\mathscr{H}}^{(N'-1)}$, the effective Hamiltonian calculated by AHT to order $N'-1$. While most of the results derived herein could, in principle, be obtained by AHT, the Floquet method provides a considerably more efficient means of determining resonance conditions and of explicitly evaluating the magnitude and phase of $-\frac{1}{2}\omega_P^{\gamma\eta}$ for specific field configurations.

C. Suppression of spiraling

For the Floquet Hamiltonian of Eq. (7), degeneracy between $|\beta,0\rangle$ and $|\alpha,n\rangle$ occurs whenever $\Delta\approx n\omega$. This corresponds to a resonance only if n, k, and l are such that the off-diagonal element of the effective Hamiltonian is nonzero. While discussion of $-\frac{1}{2}\omega_P^{\alpha\beta}$ is deferred to subsequent sections, we note here that the general stipulation $\Delta\approx n\omega$ can be exploited to define conditions under which spiraling of the magnetization in the Ω_0 frame is suppressed at resonance, without a detailed knowledge of the resonances themselves. These conditions will in turn place important constraints on the possible values of n, k, and l.

The spiraling frequency ω_s is defined as the frequency difference between the line (Ω_0) frame and the $\Omega+n\omega$ frame in which the magnetization evolves according to Eq. (14),

$$\omega_s = n\omega - \Delta . \tag{15}$$

The off-resonance part of the effective Hamiltonian is, from Eqs. (7), (12), and (13),

$$\delta_P^{\alpha\beta} = n\omega - \Delta - \frac{1}{2}\left[\frac{\omega_1^2}{\Delta+l\omega} + \frac{\omega_2^2}{\Delta+k\omega} + \frac{\omega_3^2}{\Delta-k\omega} + \frac{\omega_4^2}{\Delta-l\omega}\right], \tag{16}$$

which is zero at resonance, giving for the spiraling frequency

$$\omega_s = \frac{1}{2\omega}\left[\frac{\omega_1^2}{n+l} + \frac{\omega_2^2}{n+k} + \frac{\omega_3^2}{n-k} + \frac{\omega_4^2}{n-l}\right], \tag{17}$$

where the substitution $\Delta\approx n\omega$ is made.

In establishing circumstances under which $\omega_s=0$ at resonance, two cases are distinguished.

(i) $n=0$. The resonance condition is $\Delta=-\omega_s$, where $\omega_s=(2\omega)^{-1}[(\omega_1^2-\omega_4^2)/l+(\omega_2^2-\omega_3^2)/k)]$ by Eq. (17). In particular, if the field strengths are symmetrical about Ω,

$$\omega_1=\omega_4\equiv\omega_o, \quad \omega_2=\omega_3\equiv\omega_i \tag{18}$$

the formal resonance condition is $\Delta=0$ exactly, as diagrammed in Fig. 2, and $\omega_s=0$ at resonance regardless of ω, ω_o, and ω_i.

(ii) $n\neq 0$. The resonance condition is $\Delta=n\omega-\omega_s$, and it is apparent from Eq. (17) that $\omega_s\neq 0$ unless $l>|n|$ (or, equivalently, $|\Delta|<l\omega$, corresponding to placement of at least one rf field to each side of Ω_0).

Of the many possible degeneracies between Floquet states for four-frequency irradiation, consideration will be restricted in the following sections to that between $|\beta,0\rangle$ and $|\alpha,0\rangle$. We note that the elimination of spiraling at resonance in case (i) is more readily achieved than in case (ii), as rf fields prepared by double sideband modulation of a carrier wave at the Larmor frequency is sufficient, rather than four variably offset fields of arbitrary intensity. In addition, a smaller rf field offset Δ is required in case (i) for a given set of field intensities since $\omega_s\sim\omega(\omega_j/\omega)\ll\omega$, $1\leq j\leq 4$, placing less stringent demands on the resonance bandwidth of the rf coil.

D. Existence of the resonances: Floquet grid

For a $|\beta,0\rangle$-$|\alpha,0\rangle$ resonance to exist, $\omega_P^{\alpha\beta}$ must be nonzero; equivalently, $|\beta,0\rangle$ and $|\alpha,0\rangle$ must be connected by the off-diagonal elements of $\mathscr{H}_F$, either directly or indirectly via intermediate states. With conventional ma-

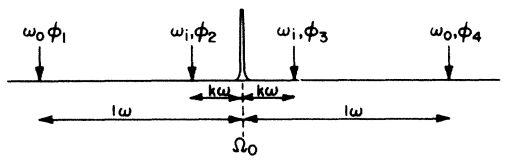

FIG. 2. A specialization of the scheme of Fig. 1, with zero offset and applied intensities symmetrical about Ω_0. For this configuration the spiraling frequency vanishes for all k, l, ω, and rf phases, as described in text.

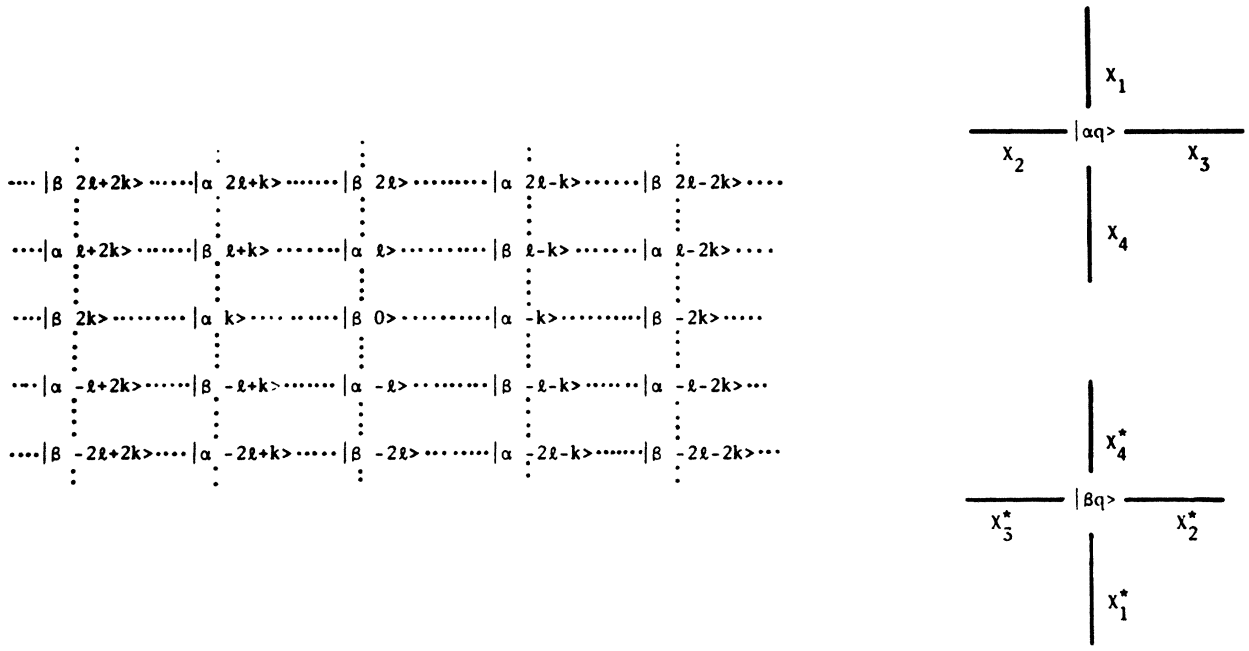

FIG. 3. (Left) Floquet-state grid in neighborhood of $|\beta,0\rangle$. (Right) Key to which solid lines connect the Floquet states when the off-diagonal elements of the Floquet Hamiltonian of Eq. (7) are nonzero.

trix representations of $\mathscr{H}_F$ it may not be obvious for given k,l whether these states are connected and, if so, what the number of intermediate states is. It is, therefore, desirable to have a representation of the Floquet states which emphasize primarily their connectivities rather than their ordering by photon number.

Consider the Floquet grid of Fig. 3. The atomic number alternates throughout the grid, while the photon number is incremented by k in one direction (here, up) and by l in the other (left). Each state is adjacent to the four states directly connected to it by the off-diagonal elements of the $\mathscr{H}_F$ of Eq. (7), and solid lines between the states are drawn if the corresponding $\omega_j \neq 0$. A necessary condition for resonance between any two states is that an uninterrupted pathway along solid lines exist between them in this grid. An analogous construction has been used in the analysis of transition pathways involved in four-wave mixing.[21]

$|\beta,0\rangle$ can be connected to $|\alpha,0\rangle$ only if the latter appears somewhere in the grid. From Eq. (7), if $|\beta,0\rangle$ is in the grid so is $|\alpha,qk+q'l\rangle$, where q and q' are any integers such that $q+q'$ is odd. Brief reflection reveals that unless $k+l$ is odd as well, a grid containing $|\beta,0\rangle$ will only contain dressed α states with odd photon numbers. (We require throughout that k and l be relatively prime.) If $k+l$ is odd, then $|\alpha,0\rangle$ must appear in the grid, since it is possible to choose $q=-l$, $q'=k$. The first prerequisite for any $|\beta,0\rangle$-$|\alpha,0\rangle$ resonance is thus

$$k+l=2m+1\ , \tag{19}$$

with m any non-negative integer.

Let us initially take $\omega_3=\omega_4=0$, $\omega_1,\omega_2\neq 0$. $|\beta,0\rangle$ is then connected to states $|\alpha,q(l-k)-k\rangle$, q any integer, and resonance with $|\alpha,0\rangle$ requires $q(l-k)-k=0$. The value $q=0$ is excluded since processes for which a single-quantum pathway exists ($k=0$, irradiation at the line frequency) are not of interest here. Also, all $q<0$ can be eliminated since $k<l$. Therefore, $l=k(q+1)/q$, $q=1,2,3,\ldots$, or, equivalently,

$$l=k+1 \tag{20}$$

for the $|\beta,0\rangle$-$|\alpha,0\rangle$ resonance induced by two fields applied to the low-frequency side of the line. This resonance is equivalent to the $(2q+1)$-photon resonance discussed in Ref. 18 for double-frequency irradiation, where the fields were situated at frequencies $k\omega$ and $k\omega(q+1)/q$ relative to the rotating-frame frequency Ω, which was in turn shifted by $\omega_s\neq 0$ from Ω_0.

The situation is illustrated using the Floquet grid in Fig. 4(a). Since the grid is periodic, only a section centered on an occurrence of the initial state $|\beta,0\rangle$ marked by a circle is needed. The nearest occurrences of $|\alpha,0\rangle$ are indicated by diamonds for $l=k+1$ (open) and $l\neq k+1$ (solid). In the former case there is one pathway along solid lines to $|\alpha,0\rangle$ which is highlighted in the figure, while in the latter no pathway exists. A similar result, illustrated in Fig. 4(b), is obtained when $\omega_1=\omega_2=0$, $\omega_3,\omega_4\neq 0$.

If $\omega_2=\omega_3=0$, $\omega_1,\omega_4\neq 0$, $|\beta,0\rangle$ is connected only to states $|\alpha,ql\rangle$ and no $|\beta,0\rangle$-$|\alpha,0\rangle$ resonance exists for $l>0$ [Fig. 4(c)]. Similarly, no resonance exists if the inner-field pair is applied alone. The remaining possible combinations of field pairs also offer no such resonance. For example [Fig. 4(d)], when $\omega_1,\omega_3\neq 0$, $|\beta,0\rangle$ is connected to states $|\alpha,q(l+k)+k\rangle$; there is no solution to the equation $q(l+k)+k=0$ for which $0<k<l$. In gen-

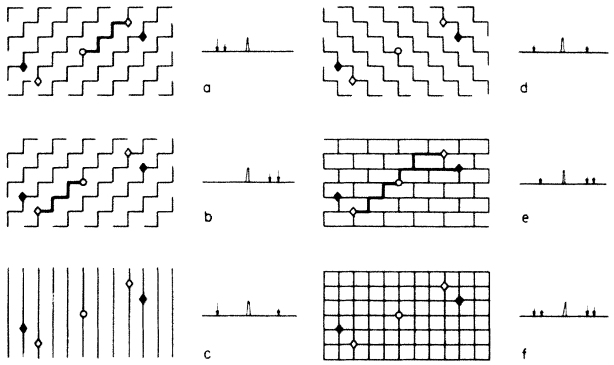

FIG. 4. Floquet-state connectivity diagrams for various irradiation schemes, indicated to the right of each diagram (not to scale). The open circle marks an occurrence of $|\beta,0\rangle$. Occurrences of $|\alpha,0\rangle$ are marked by diamonds: open if $l=k+1$ (here, $k=2$, $l=3$), or solid if $l\neq k+1$ (here, $k=1$, $l=4$). (a) $\omega_1,\omega_2\neq 0$; one pathway from $|\beta,0\rangle$ to $|\alpha,0\rangle$ if $l=k+1$, none otherwise. (b) $\omega_3,\omega_4\neq 0$; one pathway if $l=k+1$, none otherwise. (c) $\omega_1,\omega_4\neq 0$; no pathways. (d) $\omega_1,\omega_3\neq 0$; no pathways. (e) $\omega_2,\omega_3,\omega_4\neq 0$; pathways exist for all k,l compatible with Eq. (19). Multiple pathways are highlighted for $l=k+1$. (f) $\omega_1,\omega_2,\omega_3,\omega_4\neq 0$; pathways exist for all k,l compatible with Eq. (19).

eral, it is impossible for two weak rf fields applied to either side of Ω_0 to induce resonant transitions in a two-level system for any value of the terminal photon number n as long as $k>0$. If the line frequency is to lie within the frequency range delimited by the fields, then $|\Delta|<k\omega$ or, since $\Delta\approx n\omega$ at resonance, $|n|<k$. If $|\beta,0\rangle$ and $|\alpha,n\rangle$ are to be connected by the off-diagonal elements of $\mathscr{H}_F$ it is necessary that $q(l+k)+k=n$ for the field configuration of Fig. 4(d). There must then be no resonance, since this equation admits no solution for $0<|n|<k<l$.

It is apparent from Figs. 4(e) and 4(f) that if three or four fields are applied as shown, resonance between $|\beta,0\rangle$ and $|\alpha,0\rangle$ is possible, with k and l restricted only through Eq. (19). In addition, multiple pathways exist from initial to final state. The symmetrical rf field configuration of Fig. 2 therefore represents an infinite number of resonant irradiation schemes, any one of which is specified by k and l to within a scaling factor ω. In subsequent discussion, P will be replaced by k,l as the identifying subscript attached to quantities comprising the effective Hamiltonian of Eq. (11).

E. Multiphoton order of the resonances

The preceding discussion has shown that $|\beta,0\rangle$ and $|\alpha,0\rangle$ are connected by the off-diagonal elements of $\mathscr{H}_F$ for irradiation as in Fig. 2, but does not indicate the conditions under which such a resonance can be detected. Since multiple transition pathways exist [Fig. 4(f)], it is possible the sum in Eq. (9) will have a zero resultant, at least for certain choices of initial rf phases. Determining $-\frac{1}{2}\omega_{k,l}^{\alpha\beta}$ directly from $\mathscr{H}_F$ for particular values of k and l will settle the question of observability only in specific cases. An alternate approach is to formulate the overall transition process as a sequence of individual photon interactions to which fundamental conservation laws can be applied. This will permit us to determine resonance orders (without recourse to graphic devices) and to establish necessary and sufficient constraints on the rf field phases for $-\frac{1}{2}\omega_{k,l}^{\alpha\beta}$ to achieve its maximum amplitude.

We begin by defining resonance and pathway order. The multiphoton order N of a resonance is equal to the number of factors in the numerator of the first nonzero term of the perturbation expansion of $-\frac{1}{2}\omega_{k,l}^{\alpha\beta}$ in Eq. (9). This is the same as the minimum number of photons needed to complete the transition from $|\beta,0\rangle$ to $|\alpha,0\rangle$. A transition pathway of order N' is defined as a sequence of N' field interactions and $N'-1$ virtual intermediate states, beginning on $|\beta,0\rangle$, terminating on $|\alpha,0\rangle$, and conserving energy and angular momentum for the $|\beta\rangle\rightarrow|\alpha\rangle$ transition. Each term contributing to $-\frac{1}{2}\omega_{k,l}^{\alpha\beta}$ and containing $N'>N$ factors corresponds to one transition pathway of order N', and from the completeness of the Floquet states (4) Eq. (9) must contain one term for each possible pathway.

A distinction should be made between the higher-order pathway for a resonance of order N, involving $N'>N$ steps, and a more thorough diagonalization of $\mathscr{H}_F$ with application of Eq. (4). The latter refinement will incorporate high-frequency terms into $U(t)$.[18] The present treatment of four-field irradiation is restricted to first-order terms in the sence that only Eq. (14) will be used to estimate the time dependence of ρ near resonance.

In applying the conservation laws, the conclusions are independent of the reference frequency chosen for the discussion and the problem is formulated in the laboratory frame. For a transition pathway of order $N'>0$ we define the interaction numbers $n_j^{\uparrow}$ and $n_j^{\downarrow}$, $j=1,2,3,4$ as the number of absorptions from and emissions to field j, respectively, where $n_j^{\uparrow},n_j^{\downarrow}$ are non-negative integers, and assume as before that $\omega_j<\omega$ for all fields. The condition for angular momentum conservation is

$$\sum_{j=1}^{4}(n_j^{\uparrow}-n_j^{\downarrow})=1\ , \tag{21}$$

for energy conservation

$$\sum_{j=1}^{4}E_j(n_j^{\uparrow}-n_j^{\downarrow})=\Omega_0\ , \tag{22}$$

and for photon counting,

$$\sum_{j=1}^{4}(n_j^{\uparrow}+n_j^{\downarrow})=N'\ . \tag{23}$$

In Eq. (22), the photon energies are $E_1=\Omega_0-l\omega$, $E_2=\Omega_0-k\omega$, $E_3=\Omega_0+k\omega$, and $E_4=\Omega_0+l\omega$. Combining Eqs. (21) and (22) yields

$$k[(n_2^{\downarrow}+n_3^{\uparrow})-(n_2^{\uparrow}+n_3^{\downarrow})]=l[(n_1^{\uparrow}+n_4^{\downarrow})-(n_1^{\downarrow}+n_4^{\uparrow})]\ . \tag{24}$$

We are interested primarily in pathways involving the minimum number of steps as these are expected to make the largest contribution to the sum in Eq. (9). Since the

interaction numbers are non-negative and k and l are relatively prime, Eq. (24) yields two mutually exclusive constraints on the interaction numbers for minimum N':

$$n_1^{\downarrow}+n_4^{\downarrow}=k,\quad n_2^{\downarrow}+n_3^{\downarrow}=l,\quad n_1^{\uparrow}=n_2^{\downarrow}=n_3^{\uparrow}=n_4^{\downarrow}=0\ , \tag{25a}$$

$$n_1^{\uparrow}+n_4^{\uparrow}=k,\quad n_2^{\uparrow}+n_3^{\downarrow}=l,\quad n_1^{\downarrow}=n_2^{\uparrow}=n_3^{\downarrow}=n_4^{\uparrow}=0\ . \tag{25b}$$

Designating the minimum N' by N, we obtain from Eqs. (21), (23), and (25a),

$$n_1^{\uparrow}-n_2^{\downarrow}+n_3^{\uparrow}-n_4^{\downarrow}=1,\quad n_1^{\uparrow}+n_2^{\downarrow}+n_3^{\uparrow}+n_4^{\downarrow}=N\ , \tag{26}$$

which indicates that $n_1^{\uparrow}+n_3^{\uparrow}=\frac{1}{2}(N+1)$; but the interaction numbers are integral, requiring that N is odd. [An identical conclusion is reached for Eq. (25b).] Combining Eqs. (25) and (26) gives finally for the resonance order

$$N=k+l=2m+1\ , \tag{27}$$

with m any non-negative integer.

From this result, we conclude that multiphoton resonances of order 3,5,7,... are allowed for four symmetrically placed fields, where in every case the spacing parameters sum to the resonance order. Field placement for the six allowed resonances through $N=7$ is shown in Fig. 5. It should be noted from Eq. (25) that for each lowest-order pathway l photons are taken from the inner-field pair, k from the outer-field pair, and in no instance are photons both absorbed and emitted to the same field. Higher-order pathways must, in order to be compatible with Eq. (21), contain the same number of additional absorption as emission steps. Thus $N'=N+2q$, $q=1,2,3,\ldots$, and all possible pathways involve an odd number of field interactions.

F. Transition pathways of lowest order

The four nonzero interaction numbers for pathways of order $k+l$ are not completely determined by Eqs. (21)–(23), and it is possible to assign one of them, for example $n_1^{\downarrow}$ in Eq. (25a), an integer value s, $0<s<k$. Combining Eqs. (25a) and (26) then yields one set of allowed interaction numbers:

$$\begin{aligned} &n_1^{\downarrow}=s,\quad n_2^{\uparrow}=s+\tfrac{1}{2}(l-k+1)\ ,\\ &n_3^{\downarrow}=-s+\tfrac{1}{2}(l+k-1),\quad n_4^{\uparrow}=-s+k\ . \end{aligned} \tag{28}$$

The interaction numbers corresponding to Eq. (25b) are

$$\begin{aligned} &n_1^{\uparrow}=-s+k,\quad n_2^{\downarrow}=-s+\tfrac{1}{2}(l+k-1)\ ,\\ &n_3^{\uparrow}=s+\tfrac{1}{2}(l-k+1),\quad n_4^{\downarrow}=s\ , \end{aligned} \tag{29}$$

which can be obtained from Eq. (28) by exchanging subscript 1 with 4 and 2 with 3.

Each of Eqs. (28) and (29) represents for given s a number $g_{k,l}(s)$ of pathways distinguished by the order of the photon interactions. It is assumed for this two-level system that absorption and emission steps must alternate. The number of pathways is then obtained by separate permutation of the absorption and emission steps, yielding for either Eq. (28) or (29)

$$\begin{aligned} g_{k,l}(s)&=\frac{(n_1+n_3)!(n_2+n_4)!}{n_1!n_2!n_3!n_4!}\\ &=\begin{bmatrix}\frac{1}{2}(l+k+1)\\ k-s\end{bmatrix}\begin{bmatrix}\frac{1}{2}(l+k-1)\\ s\end{bmatrix}. \end{aligned} \tag{30}$$

The total number of pathways of lowest order for given k and l is then

$$G_{k,l}=2\sum_{s=0}^{k} g_{k,l}(s)=2\begin{bmatrix}k+l\\ k\end{bmatrix}. \tag{31}$$

An identical result to Eq. (31) is obtained by inspection of the Floquet grid. With one occurrence of $|\beta,0\rangle$ chosen as the origin, the closest occurrences of $|\alpha,0\rangle$ fall at $\{l,k\}$ and $\{-l,-k\}$ in the grid (Fig. 6). Every pathway of order $k+l$ between the resonant states is then confined to two rectangular regions of the grid, one in quadrant I (QI) and the other in quadrant III (QIII), each of

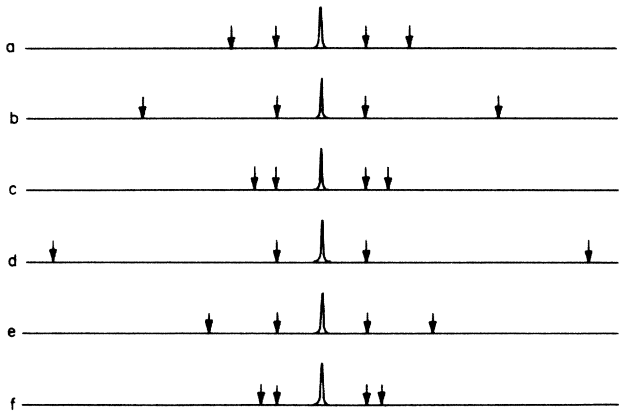

FIG. 5. Irradiation schemes for multiphoton resonances of order 3 through 7. The inner-field positions are assumed constant throughout. (a) three photons, $k=1$, $l=2$; (b) five photons, $k=1$, $l=4$; (c) five photons, $k=2$, $l=3$; (d) seven photons, $k=1$, $l=6$; (e) seven photons, $k=2$, $l=5$; (f) seven photons, $k=3$, $l=4$.

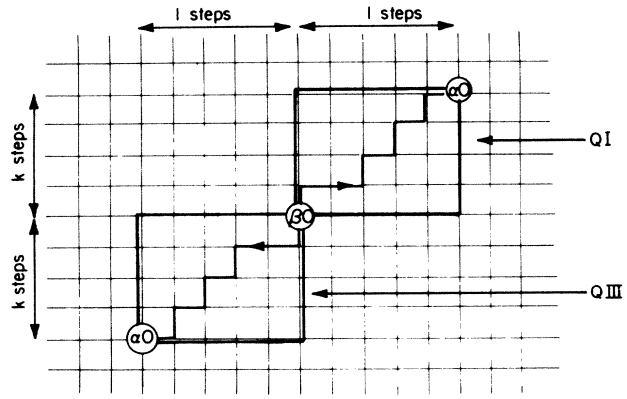

FIG. 6. Pathways of lowest order ($=k+l$) are always confined to the two regions indicated in the Floquet grid, one in the first quadrant (QI) and the other in the third quadrant (QIII). One pair of partner pathways from $|\beta,0\rangle$ to $|\alpha,0\rangle$ is highlighted.

dimension k by l steps. The number of such pathways in both quadrants is $2[(k+l)!]/(k!l!)$. QI pathways involve only absorptions (transitions out of $|\beta\rangle$) from fields 2 and 4, and emissions (transitions out of $|\alpha\rangle$) to fields 1 and 3, and thus have interaction numbers conforming to Eq. (25a). The interaction numbers of QIII pathways satisfy Eq. (25b). For every pathway in QI there is a partner in QIII obtained by inversion through the origin, with intermediate-state photon numbers related by change of signs. As discussed below, the contributions to $-\frac{1}{2}\omega_{k,l}^{\alpha\beta}$ of a pair of partners differ only in phase for the general irradiation scheme of Fig. 2.

Two limiting cases are considered briefly. If $\omega_1=\omega_2=0$ [Fig. 4(b)], $n_1^{\uparrow}=n_1^{\downarrow}=n_2^{\uparrow}=n_2^{\downarrow}=0$, and as long as $k<l$ there is no set of interaction numbers compatible with both Eqs. (21) and (28), and no QI pathway. Equation (29) is satisfied only if $l=k+1$ [compare Eq. (20)] and $s=k$, and in QIII a $g_{k,k+1}(k)=1$ pathway exists from $|\beta,0\rangle$ to $|\alpha,0\rangle$. If $\omega_1=0$ only [Fig. 4(e)] and we assume $l=k+1$ (as other choices are possible) we must have $s=0$ in Eq. (28) and $s=k$ in Eq. (29), indicating that $k+1$ QI and 1 QIII pathways of lowest order exist. This may be verified in the example shown in the figure.

G. Effective multiphoton irradiation field

We now utilize the results of Sec. II E and II F to formulate a general expression for the off-diagonal element of the effective Hamiltonian. The analysis here is limited to pathways of order $k+l$, which for weak fields make the largest contribution to the perturbation expansion of Eq. (9).

In QI, the rth pathway of order $k+l$ corresponding to a particular s value, where $1\le r\le g_{k,l}(s)$, makes a contribution to $-\frac{1}{2}\omega_{k,l}^{\alpha\beta}$,

$$w_r=\frac{X_1^s(X_2^*)^{s+(l-k+1)/2}X_3^{-s+(l+k-1)/2}(X_4^*)^{k-s}}{f_r} . \tag{32}$$

To first order f_r is the product of the differences between the resonant-state energies (represented by the average of E_0^{α} and E_0^{β}) and the Floquet-state energies of the intermediate states encountered along pathway q for the transition. For the $|\beta,0\rangle$-$|\alpha,0\rangle$ process, f_r is to first order proportional to the product of the reduced photon numbers of the intermediate states, the proportionality being exact at resonance when Eq. (18) holds.

The contribution of the partner in QIII is

$$w_r'=\frac{(X_1^*)^{k-s}X_2^{-s+(l+k-1)/2}(X_3^*)^{s+(l-k+1)/2}X_4^s}{f_r'} \tag{33}$$

and the off-diagonal element is

$$-\tfrac{1}{2}\omega_{k,l}^{\alpha\beta}=\sum_{s=0}^{k}\sum_{r=1}^{g_{k,l}(s)}(w_r+w_r') . \tag{34}$$

It is assumed in the following that Eq. (18) is satisfied in order that $\omega_s=0$ at resonance (Sec. II C). In this case $f_r=f_r'$, since the intermediate-state photon numbers differ only in sign between partner pathways and there is always an even number of intermediate states [Eq. (27)]. Combining Eqs. (8), (18), and (32)–(34) yields

$$-\tfrac{1}{2}\omega_{k,l}^{\alpha\beta}=-\frac{1}{2^{k+l}}\frac{\omega_o^k\omega_i^l}{\omega^{k+l-1}}(e^{i\Phi_{k,l}}+e^{i\Phi_{k,l}'})\times\sum_{s=0}^{k}a_{k,l}(s)e^{is(\phi_1-\phi_2-\phi_3+\phi_4)} , \tag{35}$$

where

$$\Phi_{k,l}=-k\phi_4-\frac{l}{2}(\phi_2-\phi_3)+\frac{1}{2}(k-1)(\phi_2+\phi_3) ,$$

$$\Phi_{k,l}'=-k\phi_1+\frac{l}{2}(\phi_2-\phi_3)+\frac{1}{2}(k-1)(\phi_2+\phi_3) ,$$

$$a_{k,l}(s)=\omega^{k+l-1}\sum_{r=1}^{g_{k,l}(s)}\frac{1}{f_r} .$$

From Eq. (35) it is apparent that the various transition pathways mutually interfere according to the relative initial phases of the rf fields, and that both the magnitude and phase of $-\frac{1}{2}\omega_{k,l}^{\alpha\beta}$ are sensitive to the choice of phases.

Phase constraints ensuring the maximum amplitude of $-\frac{1}{2}\omega_{k,l}^{\alpha\beta}$ for given ω, ω_o, and ω_i are next sought which amounts to finding conditions for constructive interference of all pathway contributions. We note from Eq. (35) that for the irradiation scheme of Fig. 2 the phases of every pair of partner pathways can be linked at once simply by requiring $\Phi_{k,l}=\Phi_{k,l}'+2m\pi$, or

$$k(\phi_1-\phi_4)-l(\phi_2-\phi_3)=2m\pi , \tag{36}$$

where m is any integer. It is convenient here to introduce new phase parameters $\alpha,\beta,\gamma,\delta$, given by

$$\alpha=\tfrac{1}{2}(\phi_1-\phi_4),\quad \beta=\tfrac{1}{2}(\phi_2-\phi_3) ,$$

$$\gamma=\tfrac{1}{2}(\phi_1+\phi_4),\quad \delta=\tfrac{1}{2}(\phi_2+\phi_3) , \tag{37}$$

$$\phi_1=\gamma+\alpha,\quad \phi_2=\delta+\beta,\quad \phi_3=\delta-\beta,\quad \phi_4=\gamma-\alpha ,$$

whence

$$e^{i\Phi_{k,l}}+e^{i\Phi_{k,l}'}=2e^{-i[k\gamma-(k-1)\delta]}\cos(k\alpha-l\beta) \tag{38}$$

and the first phase condition is simply

$$k\alpha-l\beta=m\pi . \tag{36'}$$

The terms within the summation in Eq. (35) represent phase differences between different pairs of partner pathways or, equivalently, between path contributions within a quadrant. It is not obvious how to link the phases of these terms because the real numbers $a_{k,l}(s)$ are not known *a priori*. The latter can be determined by a computer algorithm which generates and steps through all lowest-order pathways of one quadrant of the Floquet grid for any k,l, accumulating as it does so sums of reciprocal products of intermediate-state photon numbers for each possible value of s. When this operation is carried out, it is found in every case that the signs of the $a_{k,l}(s)$ alternate with s. Theoretical justification for this is offered below. At present, we note that the sign alternation gives the second phase condition

$$\phi_1-\phi_2-\phi_3+\phi_4=(2m+1)\pi \tag{39}$$

or

$$\delta-\gamma=(2m+1)\pi/2 , \tag{39'}$$

which together with Eq. (36) is sufficient to link constructively the phases of all pathway contributions to $-\frac{1}{2}\omega_{k,l}^{\alpha\beta}$.

When Eq. (39) is satisfied, the resultant of the terms within the summation in Eq. (35) is

$$\sum_{s=0}^{k}(-1)^s a_{k,l}(s)=S_{k,l}A_{k,l} , \tag{40}$$

where $S_{k,l}=\mathrm{sgn}[a_{k,l}(0)]$ and $A_{k,l}=\sum_{s=0}^{k}|a_{k,l}(s)|$. From the algorithm, it is found that $S_{k,l}=1$ (k odd) and $(-1)^{(l-k-1)/2}$ (k even). Selected values of $A_{k,l}$ are listed in Table I. When the two phase conditions are satisfied [taking m even in Eqs. (36') and (39')] we obtain finally for the off-diagonal element of the effective Hamiltonian, from Eqs. (35)–(40),

$$-\tfrac{1}{2}\omega_{k,l}^{\alpha\beta}=\begin{cases}(-1)^{(k+1)/2}\dfrac{\omega_o^k\omega_i^l}{(2\omega)^{k+l-1}}A_{k,l}e^{-i\gamma}, & k \text{ odd} \quad (41a)\\[2ex] (-1)^{(l+1)/2}\dfrac{\omega_o^k\omega_i^l}{(2\omega)^{k+l-1}}A_{k,l}e^{-i(\gamma+\pi/2)}, & k \text{ even} . \quad (41b)\end{cases}$$

The above relations specify, according to Eq. (11), an effective multiphoton irradiation field of magnitude

$$|\omega_{k,l}^{\alpha\beta}|=2\omega_o^k\omega_i^l A_{k,l}/(2\omega)^{k+l-1} ,$$

so that the on-resonance inversion time is

$$t_\pi=\frac{\pi}{|\omega_{k,l}^{\alpha\beta}|}=\frac{\pi(2\omega)^{k+l-1}}{2\omega_o^k\omega_i^l A_{k,l}} . \tag{42}$$

The phase of the effective field is given by

$$-\arg(\tfrac{1}{2}\omega_{k,l}^{\alpha\beta})=\begin{cases}\gamma+\dfrac{k-1}{2}\pi, & k \text{ odd} \quad (43a)\\[2ex] \gamma+\dfrac{l}{2}\pi, & k \text{ even} . \quad (43b)\end{cases}$$

For example, this field lies in the $\hat{\mathbf{x}}$ direction (phase angle equal to 0) in the Ω_0 rotating frame if $\gamma=\pi/2$ for the $k=2$, $l=3$ five-photon resonance, signifying that under on-resonance irradiation for a time $t_\pi/2$ the magnetization will nutate into $\hat{\mathbf{y}}$.

The phase conditions (36') and (39') do not unambiguously determine the four phase parameters, and for any specified phase of $-\frac{1}{2}\omega_{k,l}^{\alpha\beta}$ it is possible to choose either α or β arbitrarily. This makes possible phase cycling routines for partial suppression of rapid oscillations of the magnetization due to higher-order terms in $U(t)$ which are not included in Eq. (14). Phase cycling is considered in Sec. III B.

In order to justify the sign alternation of the $a_{k,l}(s)$ with s, two arguments are offered. The first is based on the individual transition pathways themselves. For any $s=s'$, the pathways making the largest contribution to $a_{k,l}(s')$ will be those with intermediate-state photon numbers near zero [small f_r in Eq. (32) or (34)]. Given one such dominant QI pathway for s', it is possible to derive a dominant QI pathway for $s'-1$ by replacing, between two intermediate states lying close to the resonant levels, an emit to field 1 and absorb from field 2 sequence by an emit to field 3 and absorb from field 4 sequence (Fig. 7). This new pathway differs from the old only in one intermediate state, with photon number of sign opposite to the corresponding state in the original pathway. Therefore, f_r will differ in sign between dominant pathways having s values differing by one.

A second argument is provided by average Hamiltonian theory. If $\phi_1=\phi_2=\phi_3=\phi_4$ and Eq. (18) holds, the rotating frame $\mathscr{H}(t)$ of Eq. (2) is easily shown to be self-commuting at all times; since it is also periodic with zero cycle average, every term of the Magnus expansion vanishes, as must the effective Hamiltonian in Eq. (14). (Thus no resonance is observable even if higher-order pathway contributions are included.) With $-\frac{1}{2}\omega_{k,l}^{\alpha\beta}=0$, Eq. (35) holds under assumption of equal phases only if $\sum_{s=0}^{k}a_{k,l}(s)=0$; the $a_{k,l}(s)$ thus cannot all have the same sign. Now for arbitrary choice of phases the effective Hamiltonian $\mathscr{H}_{k,l}^{\alpha\beta}$ is equivalent to $\bar{\mathscr{H}}^{(k+l-1)}$ the term calculated to order $k+l-1$ in the Magnus expansion.[20] The elements of the latter depend on the elements of the commutation $[\mathscr{H}(t),\mathscr{H}(t')]$. Recasting $\mathscr{H}(t)$ of Eq. (2) in terms of the phase parameters of Eq. (37),

TABLE I. $\log_{10}(A_{k,l})$ for multiphoton transitions.

l \ k	1	2	3	4	5	6	7	8	9
2	0.301 03								
3		−0.051 15							
4	−0.176 09		−0.766 51						
5		−0.847 03		−1.735 26					
6	−1.051 15		a		−2.899 40				
7		−1.935 17		−2.946 52		−4.222 74			
8	−2.197 30		−3.053 88		−4.261 83		−5.680 48		
9		−3.241 59		−4.348 64		b		−7.254 52	
10	−3.549 46		−4.495 82		a		−7.283 76		−9.931 08

[a]See $k=1$, $l=2$.
[b]See $k=2$, $l=3$.

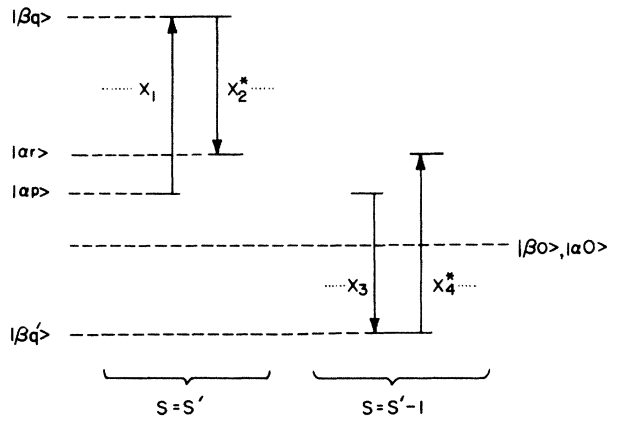

FIG. 7. Energy-level diagram (Ω_0 frame) showing three consecutive intermediate states for two dominant pathways ($|p|,|r|<l$). The preceding and following steps are represented by dots ($\cdots$) and are identical in each case. On the right an emit to field 3 and absorb from field 4 sequence replaces the emit to field 1 and absorb from field 2 sequence at left, which decrements s by 1 [Eq. (28)] and changes the sign of the photon number of the altered intermediate state.

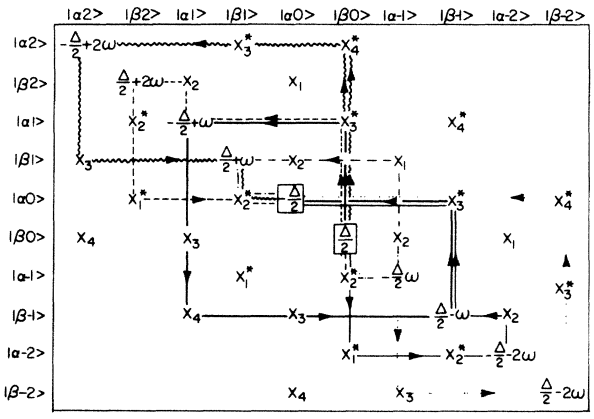

FIG. 8. Floquet Hamiltonian (partial) for $k=1$, $l=2$. Three-photon pathways from $|\beta,0\rangle$ to $|\alpha,0\rangle$ are indicated.

$$\mathscr{H}(t)=2[\,\omega_o\cos(l\omega t+\alpha)(I_x\cos\gamma+I_y\sin\gamma)+\omega_i\cos(k\omega t+\beta)(I_x\cos\delta+I_y\sin\delta)]\,,$$

we obtain after a brief calculation

$$[\mathscr{H}(t),\mathscr{H}(t')]=-4iI_z\omega_o\omega_i\sin(\delta-\gamma)\times[\cos(k\omega t+\beta)\cos(l\omega t'+\alpha)-\cos(l\omega t+\alpha)\cos(k\omega t'+\beta)]\,, \quad (44)$$

which is maximal for any t,t' only if Eq. (39') is satisfied. (When the full commutators contributing to $\hat{\mathscr{H}}^{k+l-1}$ are evaluated in any specific case, the condition on phase parameters α and β emerges as well.) Equation (44) indicates that resonances induced by the irradiation scheme of Fig. 2 vanish not only when all phases are identical, but whenever $\delta-\gamma=m\pi$ or $\phi_1-\phi_2-\phi_3+\phi_4=2m\pi$, m any integer.

H. Explicit calculation for three-photon resonance

The lowest-order multiphoton resonance induced by four-frequency irradiation is the three-photon resonance for $k=1$, $l=2$ [fields as in Fig. 3(a)]. A portion of $\mathscr{H}_F$ is displayed in Fig. 8. A total of six pathways connect $|\beta,0\rangle$ and $|\alpha,0\rangle$ via the minimum number $N=3$ steps, in agreement with Eq. (31). These are shown schematically for the laboratory frame in Fig. 9. Two of then, involving only the upper or lower field pair, resemble three-photon pathways for double-frequency irradiation applied above or below Ω. A direct calculation from Eqs. (7) and (9) yields

$$-\tfrac{1}{2}\omega_{1,2}^{\alpha\beta}=\frac{1}{8\omega^2}(\,\omega_1\omega_2\omega_3 e^{i(-\phi_1+\phi_2-\phi_3)}+\omega_2\omega_3\omega_4 e^{i(-\phi_2+\phi_3-\phi_4)}-\omega_1\omega_2^2 e^{i(\phi_1-2\phi_2)}-\omega_3^2\omega_4 e^{i(\phi_4-2\phi_3)})\,. \quad (45)$$

Applying Eqs. (18) and (37),

$$-\tfrac{1}{2}\omega_{1,2}^{\alpha\beta}=-i\frac{\omega_o\omega_i^2}{2\omega^2}e^{-i\delta}\sin(\delta-\gamma)\cos(\alpha-2\beta)\,. \quad (46)$$

When conditions (36') and (39') are satisfied for m even ($\delta=\gamma+\pi/2$),

$$-\tfrac{1}{2}\omega_{1,2}^{\alpha\beta}=-\frac{\omega_o\omega_i^2}{2\omega^2}e^{-i\gamma}\,,$$

as consistent with Eq. (41a). The maximum amplitude of the three-photon effective field [Eq. (11)] is then

$$|\,\omega_{1,2}^{\alpha\beta}\,|_{\max}=\frac{\omega_o\omega_i^2}{\omega^2}\,. \quad (47)$$

There are 52 pathways of order 5, which make a maximum contribution to the magnitude of the effective field of

$$|\,\omega_{1,2(5)}^{\alpha\beta}\,|_{\max}=\frac{\omega_o\omega_i^2}{\omega^2}\left[\frac{4\omega_i^2-5\omega_o^2}{24\omega^2}\right], \quad (48)$$

as determined from the Floquet grid. The latter quantity

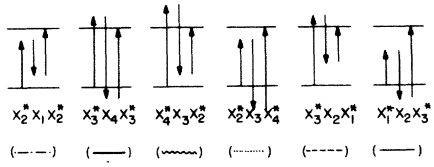

FIG. 9. The six three-photon pathways from $|\beta,0\rangle$ to $|\alpha,0\rangle$ for $k=1$, $l=2$ represented diagrammatically in the laboratory frame.

will be relatively small if $\omega_o, \omega_i < \omega$. The 526 pathways of order 7 make a still smaller contribution. The numerical importance of higher-order pathways as a function of rf field strength will be assessed below.

I. Comparison of two-field irradiation

The response of a spin-$\frac{1}{2}$ system to double-frequency irradiation has been extensively characterized.[1-18] The salient differences between this and the response to four fields are as follows.

(i) Resonances exist with four fields for any k and l such that Eq. (27) is satisfied, while with two fields only $l = k + 1$ is possible. The on-resonance effective field in each case depends in a unique way on the intensities and initial phases of the inner- and outer-field pairs [Eqs. (38) and (41)].

(ii) Many mutually interfering pathways exist for any resonance induced by four-frequency irradiation, as opposed to a single pathway in the case of the two rf fields. The effective multiphoton irradiation field for four symmetrically applied rf fields thus cannot be regarded as a superposition of two effective fields produced by rf field pairs applied above and below Ω_0; the actual intensity can be greater or less than that predicted by superposition, and the phase is essentially unrelated. Taking the three-photon resonance as an example, the effective field magnitude for a pair of rf fields applied below Ω_0 is[18]

$$|\omega_3^{\alpha\beta}| = \frac{\omega_o \omega_i^2}{4\omega^2} .$$

Variation of the phase of one of the rf fields alters the phase, but not the amplitude, of $\omega_3^{\alpha\beta}$. An identical result is obtained if the field pair is applied above Ω_0. For four-frequency irradiation, on the other hand, the amplitude of the effective multiphoton field is highly dependent on the initial rf field phases [Eq. (46)] and can achieve a maximum amplitude [Eq. (47)] twice that expected by simple superposition.

In general, the maximum amplitude of the effective field is significantly greater for given applied rf power with four-frequency irradiation. Systematic development of $\mathscr{H}_F$ in the two-field case gives

$$|\omega_N^{\alpha\beta}|_{\text{max, 2 fields}} = \frac{\omega_o^{(N-1)/2}\omega_i^{(N+1)/2}}{(2\omega)^{N-1}\{[(N-1)/2]!\}^2} , \quad (49)$$

where ω is the interfield spacing, while for four fields with $k = (N-1)/2$, $l = (N+1)/2$ we have from Eq. (41),

$$|\omega_N^{\alpha\beta}|_{\text{max, 4 fields}} = \frac{2\omega_o^{(N-1)/2}\omega_i^{(N+1)/2}}{(2\omega)^{N-1}} A_{(N-1)/2,(N+1)/2} . \quad (50)$$

Equations (49) and (50) are compared for the same total rf field intensity by halving the values of ω, ω_o, and ω_i in the four-field case. The requirement that ω be scaled is made so that the two calculations hold to approximately the same degree of accuracy within the first-order theory. A ratio R is then calculated which gives the effective enhancement achieved by four fields:

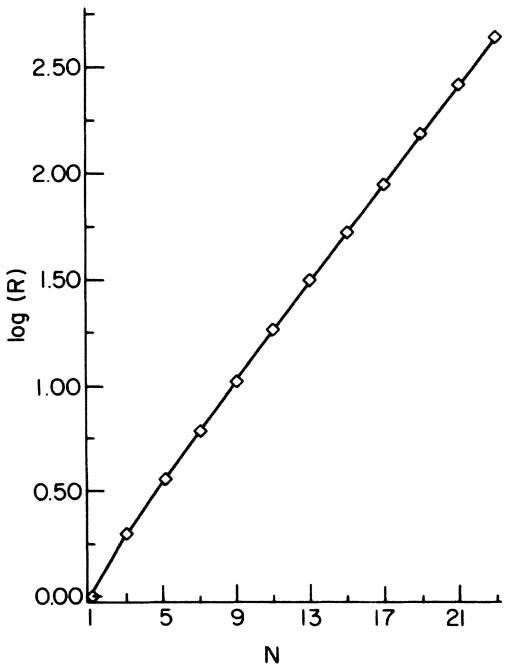

FIG. 10. Graph of log$R$ vs photon number N. R, given by Eq. (51), is the ratio of the maximum effective multiphoton irradiation field for four fields to that for two fields, normalized to the same total applied rf intensity.

$$R = \{[(N-1)/2]!\}^2 A_{(N-1)/2,(N+1)/2} . \quad (51)$$

R is graphed against N in Fig. 10. It is greater than unity for all $N > 1$ and increases logarithmically with N for large N.

(iii) Spiraling can be eliminated for four-frequency irradiation by requiring the field positions and intensities to be symmetrical about Ω_0 (Sec. II C); in contrast, resonance is forbidden for two weak fields placed to either side of Ω_0 for spin $I = \frac{1}{2}$, and all multiphoton resonances induced by two fields must involve spiral motion of the magnetization with respect to the Larmor frame.

Because of the cancelation of second-order effects associated with spiraling, the potential enhancement achievable for $N = 3$ is larger than the value of 2 given by Eq. (51). The rf field intensities cannot be augmented without limit unless the field separations are increased proportionally; otherwise, rapid motion of the magnetization vector about the instantaneous field direction dominates the multiphoton procession of Eq. (14) to the extent that it is no longer meaningful to define an effective multiphoton field or t_π.[18] One criterion for defining a limiting inner rf field intensity $\omega_{i,\max}$ for $N = 3$ is $\omega_{i,\max} = \Omega_0 - \Omega_i$, where Ω_i is the inner-field frequency. Since $\Omega - \Omega_i = \omega$ and $\Omega - \Omega_0 = \omega_s$ [Fig. 1; Eq. (15)], we find

$$\omega_{i,\max} = \omega - \omega_s . \quad (52)$$

For two fields ($\omega_3 = \omega_4 = 0$), $\omega_s = (\omega_o^2 + 2\omega_i^2)/4\omega$ from Eq. (17); setting $\omega_o = \omega$ and $\omega_i = \omega_{i,\max}$, Eq. (52) gives

$\omega_{i,\max}=\omega(\sqrt{10}/2-1)$. Defining the total rf intensity $W=\omega_0+\omega_i$, Eq. (49) yields a maximum $|\omega_3^{\alpha\beta}|=0.25W(7/\sqrt{10}-2)=0.053W$ when the intensities are pushed to the limit for given ω. For symmetric four-field irradiation $\omega_s=0$, $\omega_{i,\max}=\omega$, and from Eq. (50) $|\omega_3^{\alpha\beta}|_{\max}=0.25W$ at this limit.

J. Form of resonant rf irradiation

It was shown in Sec. II C that the rf field configuration necessary for resonance without spiraling was as shown in Fig. 2, with irradiation frequencies and intensities symmetric about Ω_0. Restrictions on the rf phases were in turn given by Eqs. (36) and (39) in Sec. II G. The form of rf field required for resonant excitation satisfying Eq. (18) is

$$\mathbf{B}_{\rm rf}=2\hat{\mathbf{x}}\{\omega_1\cos[(\Omega_0-l\omega)t-\phi_1]+\omega_2\cos[(\Omega_0-k\omega)t-\phi_2]+\omega_3\cos[(\Omega_0+k\omega)t-\phi_3]+\omega_4\cos[(\Omega_0+l\omega)t-\phi_4]\}\ .$$

Letting $\epsilon\equiv\delta-\gamma$,

$$\mathbf{B}_{\rm rf}=4\hat{\mathbf{x}}\{\cos(\Omega_0t-\gamma)[\omega_o\cos(l\omega t+\alpha)+\omega_i\cos\epsilon\cos(k\omega t+\beta)]+\sin(\Omega_0t-\gamma)[\omega_i\sin\epsilon\cos(k\omega t+\beta)]\}\ .$$

If $\epsilon=0$, $\mathbf{B}_{\rm rf}$ has the form of a purely amplitude-modulated wave oscillating at frequency Ω_0. It was shown through Eq. (44), however, that no multiphoton resonance can be detected for this phase choice, and phase modulation must be necessary as well. Taking a value of $\pi/2$ for ϵ and $\alpha=l\theta$, $\beta=k\theta$ [Eqs. (36′) and (39′)] we get for the optimum rf field

$$\mathbf{B}_{\rm rf}=4\hat{\mathbf{x}}[\omega_o\cos(\Omega_0t-\gamma)\cos(l\omega t+l\theta)+\omega_i\sin(\Omega_0t-\gamma)\cos(k\omega t+k\theta)]\ . \quad (53)$$

The requisite high-frequency waves of Eq. (53) can be obtained by initially phase shifting the carrier by γ radians relative to the reference wave and subsequently dividing this into unshifted and $\pi/2$ phase-shifted parts. γ determines the phase of the effective multiphoton field [Eq. (43)] and need not be varied in phase-cycling routines. The pair of derived high-frequency waves are each amplitude modulated by a phase-shifted low-frequency oscillation, as indicated in Eq. (53), and attenuated to obtain a desired ω_o/ω_i. The phases of the modulation waves are relative to the reference wave at time $t=0$. The experimental implementation of Eq. (53) through carrier wave modulation is in progress in this laboratory.

III. COMPUTER SIMULATIONS

A. Procedure

In order to establish the extent to which the theory outlined in the preceding sections actually describes the motion of an ensemble of noninteracting spins $\frac{1}{2}$ under four-frequency irradiation, numerical simulation of the time evolution of the magnetization **M** was performed. This entailed iterative evaluation of Eq. (3) using the exact time-dependent Hamiltonian.[19] In the present study, the evaluation of $\rho(t)$ is initially performed in the Ω rotating frame (Fig. 1) in which $\rho(t)$ is periodic. Since for Δt small and fixed,

$$U(t+\Delta t;t)\approx\exp[-i\mathcal{H}(t)\Delta t]=\exp[-i\mathcal{H}(t+T)\Delta t]\approx U(t+T+\Delta t;t+T)\ ,$$

where $T=2\pi/\omega$, it is necessary only to assemble a table of values of U over a single period T, rather than reevaluate U after every time increment Δt for the entire spin evolution time. Typically, calculations with $T/\Delta t$ between 100 and 2000 gave limiting accuracy. To obtain $\rho(t)$ in another frame rotating at frequency Ω', the transformation

$$\rho'(t)=e^{-i\omega' tI_z}\rho(t)e^{i\omega' tI_z}$$

is applied, with $\omega'=\Omega'-\Omega$.

B. The three-photon resonance

Figure 11 exhibits the motion of **M** in the Larmor frame calculated numerically when the three-photon resonance condition is satisfied. Separate pairs of fields cannot invert **M**, inducing instead a period wobble about $\hat{\mathbf{z}}$. The failure of two fields to one side of Ω_0 to induce a

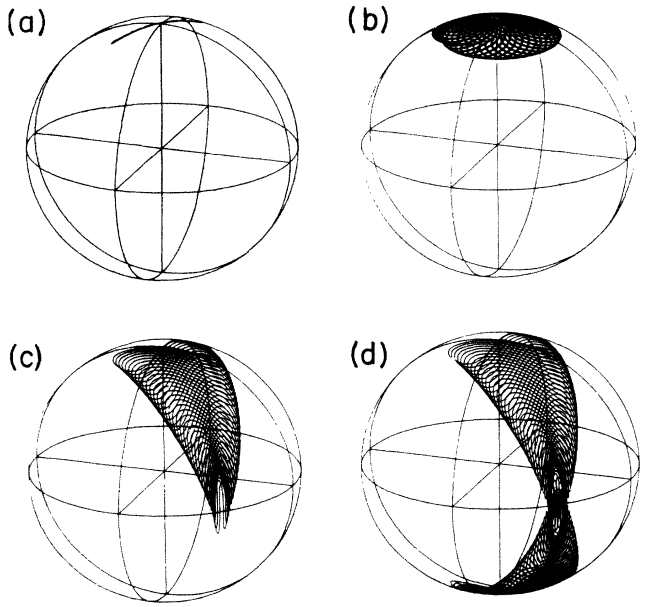

FIG. 11. Calculated motion of magnetization vector during multifrequency irradiation; $k=1$, $l=2$ (three-photon resonance). In each case $\alpha=\beta=0$, $\gamma=-\pi/4$. In this and all subsequent simulations, the phase parameter δ is fixed by $\delta=\gamma+\pi/2$ [Eq. (39′)]. (a) $\nu_1=\nu_4=0$, $\nu_2=\nu_3=4$ kHz, $t=3.21$ ms; (b) $\nu_3=\nu_4=0$, $\nu_1=\nu_2=4$ kHz, $t=3.21$ ms; (c) $\nu_1=\nu_2=\nu_3=\nu_4=4$ kHz, $t=1.61$ ms; (d) as in (c), $t=3.21$ ms.

transition is not unexpected, since with $\Delta=0$ we are far from the three-photon resonance condition for this field configuration. When the four fields are applied simultaneously as indicated, a π pulse of 3.2 ms is administered, comparing favorably with a figure of 3.125 ms predicted by Eq. (42). Spiral motion is absent and the phase of the resonance is in agreement with Eq. (43a). The exact motion contains a high-frequency component of period $2\pi/\omega$ superimposed on the simple nutation given by Eq. (14); this is a manifestation of higher-order terms in $U(t)$ in Eq. (4). The apparent focusing of **M** in the transverse plane is, as will be seen from subsequent simulations, a general characteristic of multiphoton resonances induced by four symmetrically placed fields.

The evolution of M through a fixed time period (equivalent to t_π at resonance) as the separation of the outer fields is varied is shown in Fig. 12. The inner-field separations are fixed at ± 20 kHz from Ω_0. Appreciable nutation of **M** away from $\hat{\mathbf{z}}$ occurs only when the outer-field separation is within 100 Hz of the resonance value of 30 kHz. Thus despite the fact that rf field strengths of 4 kHz were employed in this simulation, the resonance width is only of the order of $\omega_{1,2}^{\alpha\beta}$, here 156 Hz.

In Fig. 13, the variation of the π-pulse time with the rf field intensities and initial phases is graphed. The curves in Fig. 13(a) represent the prediction according to Eq. (42), while in Fig. 13(b) a correction for transition pathways of order 5 and 7 is included. The points give the numerically determined inversion times. The results confirm the dependence of $|\omega_{1,2}^{\alpha\beta}|$ on the first power of ω_0

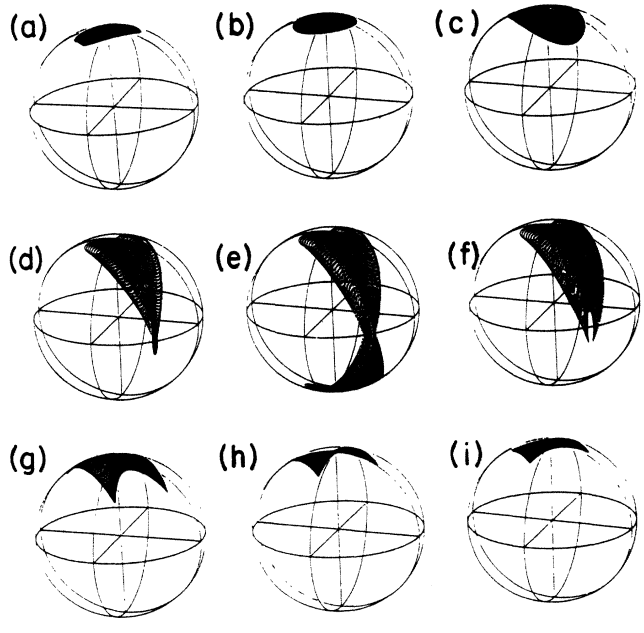

FIG. 12. Motion of magnetization near three-photon resonance: outer-field separation varied, inner-field separation constant at 40 kHz. For each plot $\alpha=\beta=0$, $\gamma=-\pi/4$, $\nu_j=4$ kHz for all j, $t=3.21$ ms. The outer-field separations are (a) 86 kHz, (b) 82 kHz, (c) 80.6 kHz, (d) 80.2 kHz, (e) 80 kHz, (f) 79.8 kHz, (g) 79.4 kHz, (h) 78 kHz, and (i) 74 kHz. Axes as in Fig. 8(a).

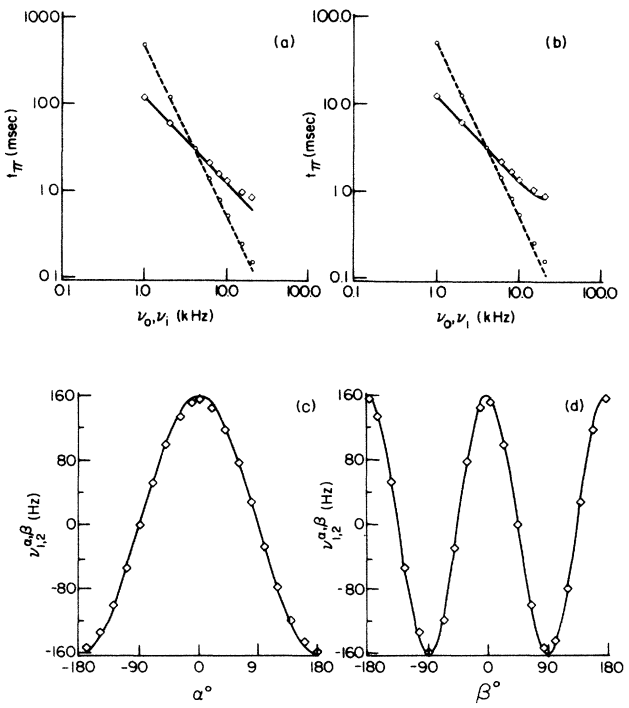

FIG. 13. (a) and (b) Variation of π-pulse time with field strength for three-photon ($k=1$, $l=2$) resonance. One field intensity is varied, the other fixed at 4 kHz. In each case $\nu=\omega/2\pi=20$ kHz. Symbols, numerically determined t_π; ◇, ν_0 variable; ○, ν_i variable. Lines, theoretical t_π including (a) three- or (b) three-, five-, and seven-photon pathways: ——, ν_0 variable; — — —, ν_i variable. (c) and (d) Variation of $|\nu_{1,2}^{\alpha\beta}|$ with phase parameters α and β. In each case $\nu=20$ kHz, $\nu_i=\nu_0=4$ kHz. Symbols are numerically determined values. Lines are from Eq. (41). (c) $\beta=0$, α varied; (d) $\alpha=0$, β varied.

and the second power of ω_i, and show clearly [Figs. 13(c) and 13(d)] that of the period of the modulation of $|\omega_{1,2}^{\alpha\beta}|$ by the inner phase parameter β is half that the outer phase parameter α [Eq. (46)]. As the rf field intensities approach ω the first-order prediction becomes less accurate, although inclusion of higher-order pathways improves agreement for $\omega_o \sim \omega$.

Phase cycling with coherent averaging can be employed to suppress much of the high-frequency motion of **M**. Figures 14(a)—14(d) show the evolution of **M** viewed along z for four sets of phase parameters α and β such that $\alpha-2\beta=2m\pi$. Each set may be regarded as a step of a phase cycle in which α and β are successively incremented by π and $\pi/2$, respectively (Table II). Figure 14(e) plots $\mathbf{M}_{av}$, the average magnetization for the four-step cycle (for convenience of presentation, phase was decreased by $\pi/4$ in this calculation) showing virtually none of the rapid motion of Fig. 11(b). A low-amplitude residual oscillation of $\mathbf{M}_{av}$ results from cancellation of magnetization components during averaging. Consideration of the importance of phase cycling raises the question of detecting of multiphoton resonances in general. A spin evolution diagram as thus far presented does not represent a single acquisition. To determine the motion of **M** over a

period of time t for one set of irradiation parameters a series of acquisitions must be taken, where the time t_1 of multifrequency irradiation is varied ($0<t_1<t$) and the magnetization $\mathbf{M}(t_1,t_2)$ phase-sensitivity sampled for each t_1 value as a free induction decay during time t_2 after switching off the rf fields. Fourier transformation over the second time domain permits reconstruction of $\mathbf{M}(t_1)$ as a projection in the transverse plane. To enhance the signal to noise ratio the results of multiple acquisitions for each t_1 value would ordinarily be averaged. If the phase parameters remain the same for all acquisitions, $\mathbf{M}(t_1)$ will appear smeared over a substantial region of the transverse plane. Figure 14(e) shows that additional improvement is possible when successive acquisitions are carried out with cycling of phase parameters α and β, particularly when accurate measurement of the nutation and phase angles of $\mathbf{M}$ are desired.

The problem of offsets and spiral motions is considered in Figs. 15 and 16. The coefficient of I_z in the effective Hamiltonian is, from Eq. (16),

$$\omega_{\text{off}}=-\Delta\left[1-\frac{1}{4\omega^2}(\omega_o^2+4\omega_i^2)\right],$$

where we assume $\Delta\ll\omega$. In the Ω rotating frame, $\mathbf{M}$ precesses about an effective field of magnitude

$$2\pi\nu_{\text{eff}}=(|\omega_{1,2}^{\alpha\beta}|^2+\omega_{\text{off}}^2)^{1/2}. \tag{54}$$

The precession frequency is just ν_{eff} and is determined readily from projection plots of the calculated motion of $\mathbf{M}$; $|\omega_{1,2}^{\alpha\beta}|$ is calculated from Eq. (42) at resonance. Figure 15 shows that the variation of the numerically derived ν_{eff}, as ascertained from the precession frequency, with $\Delta/2\pi$ is in close agreement with the prediction of Eq. (54) (solid line). The dashed line graphs the semiclassical relation

$$2\pi\nu_{\text{eff}}=(|\omega_{1,2}^{\alpha\beta}|^2+\Delta^2)^{1/2},$$

which lacks the correlation for the level shifts and agrees less precisely with the numerical determinations.

The calculated motion of the spins in the Ω_0 frame when the field intensities are not symmetrical is given in Figs. 16(a) and 16(b). Because $n=0$ and the field positions are centered on the line frequency ($\Delta=0$), we have from Eq. (15) $\omega_s=0$. However, the irradiation is not on resonance; from Eq. (16) the resonance condition for the given set of parameters is $\Delta=122$ Hz. The calculated motion shows, as expected from Eqs. (45) and (16), simple precession about an effective field which is the resultant of on- and off-resonance components equal to

$$-\hat{\mathbf{y}}(\omega_2+\omega_3)(\omega_1\omega_2+\omega_3\omega_4)/4\omega^2$$

and

$$\hat{\mathbf{z}}[\omega_1^2-\omega_4^2+2(\omega_2^2-\omega_3^2)]/4\omega,$$

respectively. It is possible to invert the magnetization

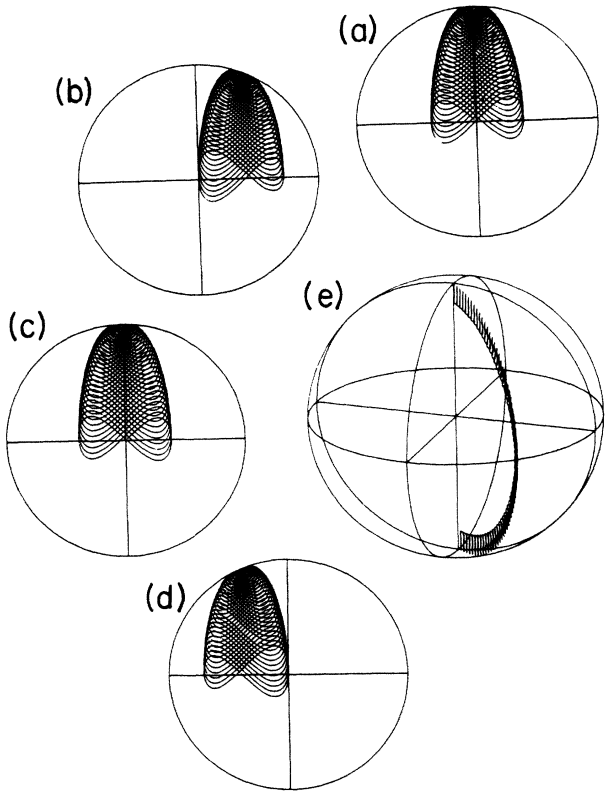

FIG. 14. Motion of spins at three-photon resonance. Irradiation parameters in kHz are as in Fig. 12(e). (a)–(d) phase $\gamma=0°$; (e) phase $\gamma=-\pi/4$ for clarity. (a) $\alpha=0$, $\beta=0$; (b) $\alpha=\pi$, $\beta=\pi/2$; (c) $\alpha=0$, $\beta=\pi$; (d) $\alpha=\pi$, $\beta=-\pi/2$; (e) average of (a)–(d).

TABLE II. Phase cycles for multiphoton resonances. In each case γ is chosen so that the effective multiphoton irradiation field lies along $\hat{\mathbf{x}}$, and $\delta=\gamma+\pi/2$.

	ϕ_1	ϕ_2	ϕ_3	ϕ_4	α	β	γ
$k=1,\ l=2$	x	y	y	x	0	0	0
	$-x$	$-x$	x	$-x$	π	$\pi/2$	0
	x	$-y$	$-y$	x	0	π	0
	$-x$	x	$-x$	$-x$	π	$-\pi/2$	0
$k=2,\ l=3$	y	$-x$	$-x$	y	0	0	$\pi/2$
	$-x$	x	x	x	$\pi/2$	π	$\pi/2$
	$-y$	$-x$	$-x$	$-y$	π	0	$\pi/2$
	x	x	x	$-x$	$-\pi/2$	π	$\pi/2$

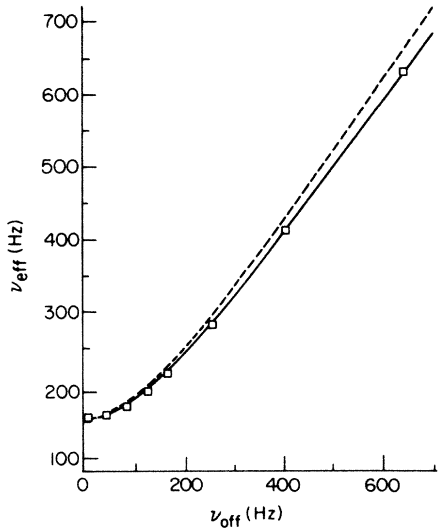

FIG. 15. Variation of effective field magnitude with offset for the three-photon ($k=1$, $l=2$) resonance. The offset of the center of the irradiation pattern relative to the line frequency is varied. The field intensities are 4 kHz and $\omega/2\pi=20$ kHz. Symbols are values of ν_{eff} determined numerically; ν_{eff} is the inverse of the precession period calculated in the Ω frame. Solid line is graph of Eq. (54), with three-photon effective field strength as predicted by first-order Floquet theory. Dashed line is as the preceding, but neglecting second-order corrections to Floquet-state energies arising from nonzero offset.

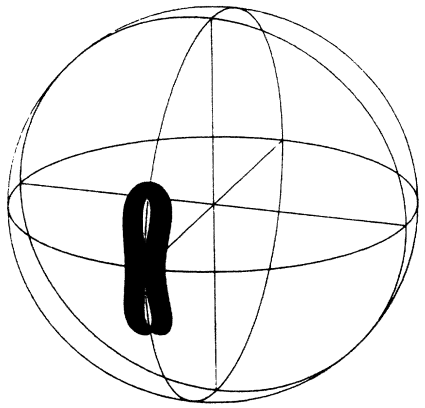

FIG. 17. Motion of magnetization for the three-photon ($k=1$, $l=2$) resonance following a $-\pi/2$ pulse applied along y. The field intensities are 4 kHz and $\omega/2\pi=20$ kHz. Phases $\alpha=\beta=\gamma=0$; $t=6.4$ ms.

only if the rf fields are given an offset of 122 Hz relative to Ω_0, as indicated in Fig. 16(c), but Δ is then nonzero and the magnetization exhibits spiral motion. As a final illustration, if the field intensities are symmetrical about Ω and Δ is nonzero, we have both off-resonance irradiation and an effective Hamiltonian which is time independent in a frame differing from that of the line, and the calculated magnetization executes combined off-resonance precession and spiral motion [Fig. 16(d)].

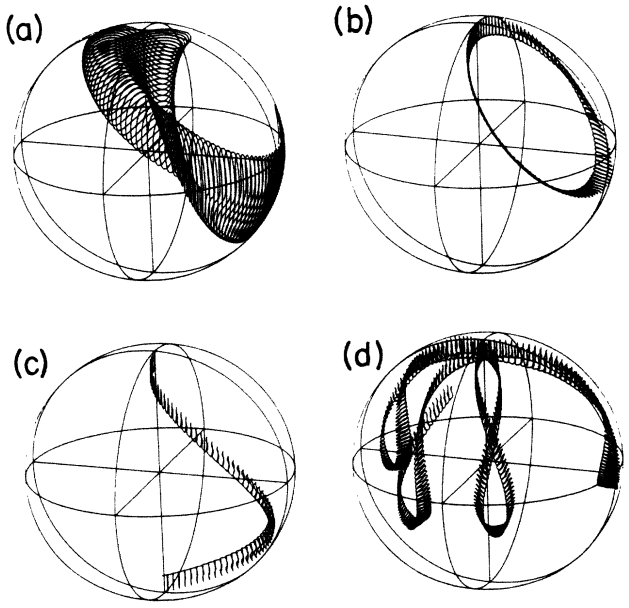

FIG. 16. Motion of magnetization for the three-photon ($k=1$, $l=2$) resonance. In each case $\omega/2\pi=20$ kHz, $\alpha=\beta=0$, $\gamma=-\pi/2$. (a) Field intensities not symmetric, zero offset; $\nu_1=\nu_2=3.8$ kHz, $\nu_3=\nu_4=4.2$ kHz, $t=3.2$ ms. (b) As in (a), with phase cycling, $t=6.4$ ms. (c) As in (a), with phase cycling, offset equal to 122 Hz. (d) All field intensities are 4 kHz, offset equal to 122 Hz, $t=20$ msec, with phase cycling.

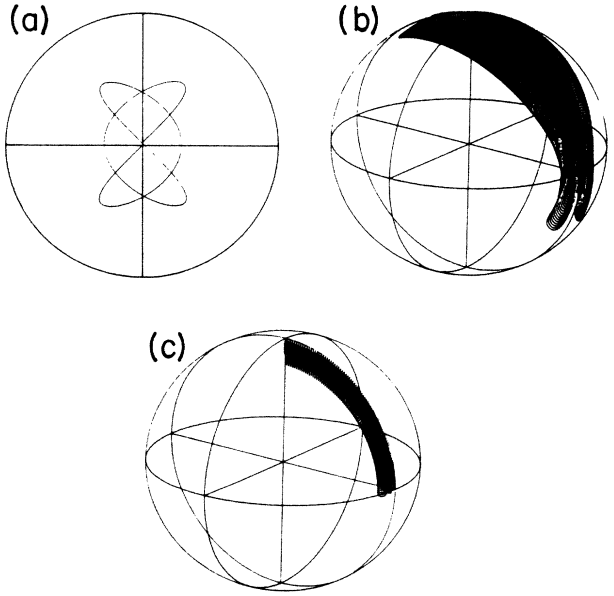

FIG. 18. Calculated motion of magnetization for the five-photon ($k=2$, $l=3$) resonance. All field strengths are 10 kHz, phases $\alpha=\beta=0$, $\gamma=\pi/2$. (a) $t=0.05$ ms, projection in xy plane; (b) $t=4.0$ ms; (c) $t=4.0$, with phase cycling (Table II).

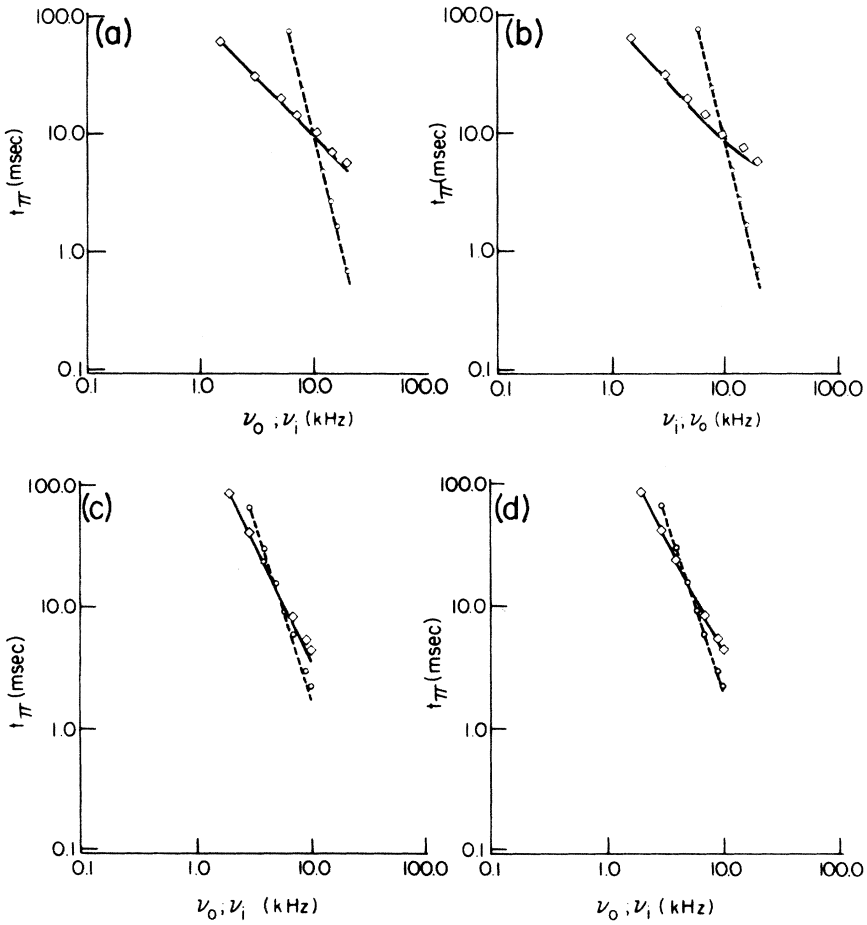

FIG. 19. (a) and (b) Variation in π-pulse time with field strength for five-photon ($k=1$, $l=4$) resonance. One field intensity is varied, the other fixed at 10 kHz. In each case $\nu=\omega/2\pi=20$ kHz. Symbols, numerically determined t_π: ◇, ν_0 variable; ○, ν_i variable. Lines, theoretical t_π including (a) five- or (b) five- and seven-photon pathways: ——, ν_0 variable; — — —, ν_i variable. (c) and (d) As in (a) and (b), respectively, for $k=2$, $l=3$ resonance. One field intensity is varied, the other fixed at 5 kHz. In each case $\nu=10$ kHz.

It has been assumed to this point that **M** initially lies parallel to $\hat{\mathbf{z}}$. Figure 17 depicts the computed motion of the spins under resonant four-frequency irradiation providing a three-photon effective field of 156 Hz along $\hat{\mathbf{x}}$, applied after an initial $\pi/2$ pulse along $-\hat{\mathbf{y}}$ which rotated **M** into $\hat{\mathbf{x}}$. The magnetization is locked in the rotating frame using only off-resonance rf fields.

C. The five- and seven-photon resonances

The calculated motion of **M** for the five-photon ($k=2$, $l=3$) resonance is shown in Fig. 18(a). **M** nutates into $+\hat{\mathbf{y}}$, indicating that the effective five-photon field lies along $\hat{\mathbf{x}}$, as consistent with Eq. (43b) ($\gamma=\pi/2$). The calculated $\pi/2$ pulse time of 4.0 ms may be compared with a value of 3.6 ms from Eq. (42) and of 3.8 ms from

$$|\omega_{2,3}^{\alpha\beta}| = \frac{\omega_0^2\omega_i^3}{\omega^4}\left[\frac{1}{9}-\frac{\omega_i^2+1.912\omega_o^2}{120\omega^2}\right],$$

which includes seven-photon pathways. A cycle of the high-frequency motion, as viewed along the $\hat{\mathbf{z}}$ axis at the start of four-field irradation, is shown in Fig. 18(b), while Fig. 18(c) illustrates the extent to which this motion can be suppressed by phase cycling. The phase cycle used here differs from that for $k=1$, $l=2$ (Table II) in that the roles of parameters α and β are reversed.

To establish that the number of interactions of the spin with the inner and out rf field pairs are indeed different for the two possible five-photon resonances, the variation of t_π with rf field intensity is graphed in Fig. 19 for $k=1$, $l=4$ and $k=2$, $l=3$. In each case the numerically determined values fall very close to lines of slope $-l$ (inner-field strength varied) or $-k$ (outer-field strength varies) on a double logarithmic plot, as predicted by Eq. (42) and the general discussion of Sec. II E.

Agreement between the theory and calculation is somewhat improved for rf field intensities approaching ω if seven-photon pathways are included in $-\frac{1}{2}\omega_{k,l}^{\alpha\beta}$. It is noteworthy that π-pulse times of the order of 1 ms are achievable with $\omega_o,\omega_i<\omega$, and $\omega/2\pi\approx 10$ kHz.

The coherence phase angles for the various multiphoton

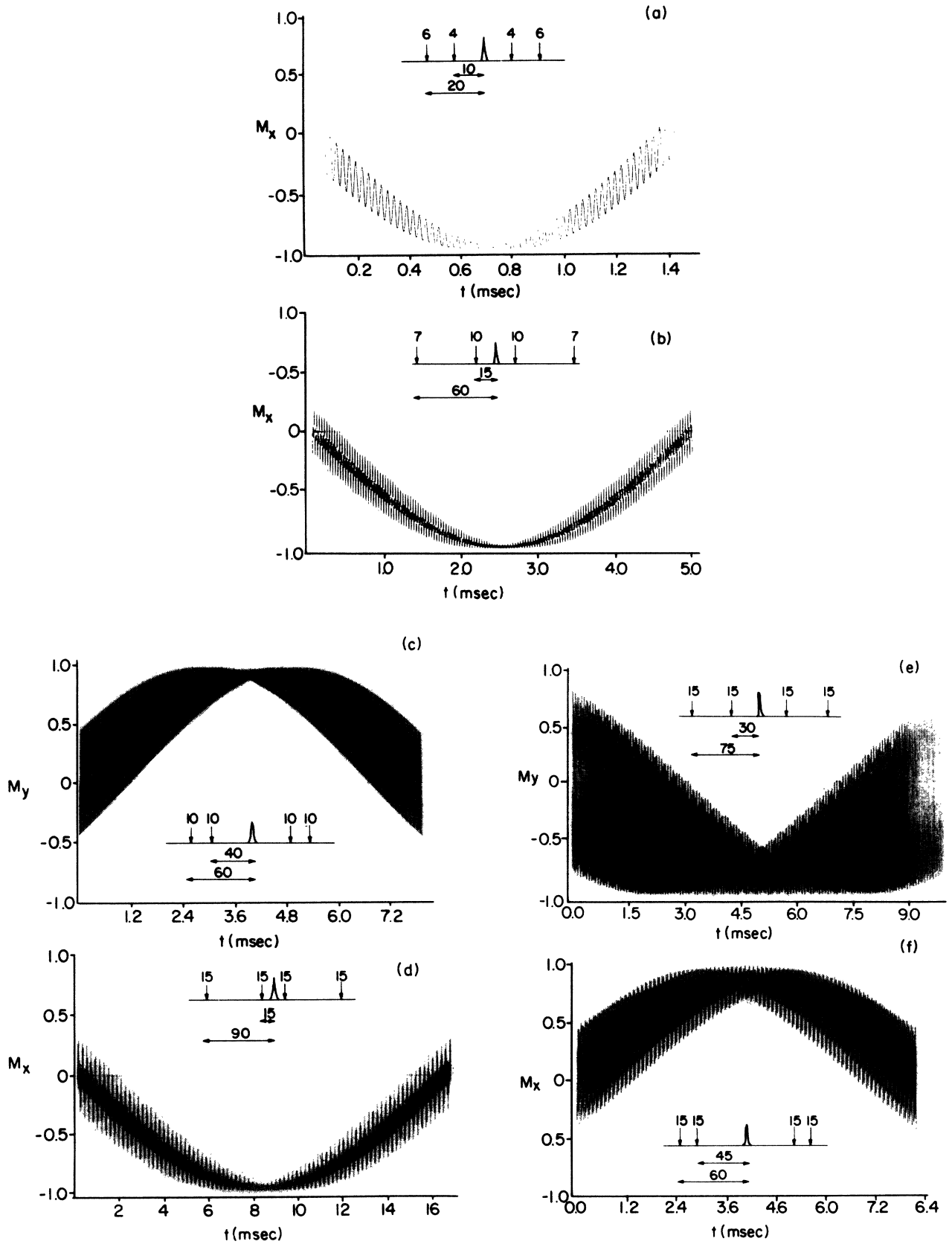

FIG. 20. Calculated resonant compound of the magnetization for multiphoton resonances from $N=3$ to 7. The field separations and intensities (in kHz) are indicated in the figure. In each case $\alpha=\beta=0$, $\gamma=\pi/2$. (a) Three photons, $k=1$, $l=2$; (b) five photons, $k=1$, $l=4$; (c) five photons, $k=2$, $l=3$; (d) seven photons, $k=1$, $l=6$; (e) seven photons, $k=2$, $l=5$; (f) seven photons, $k=3$, $l=4$.

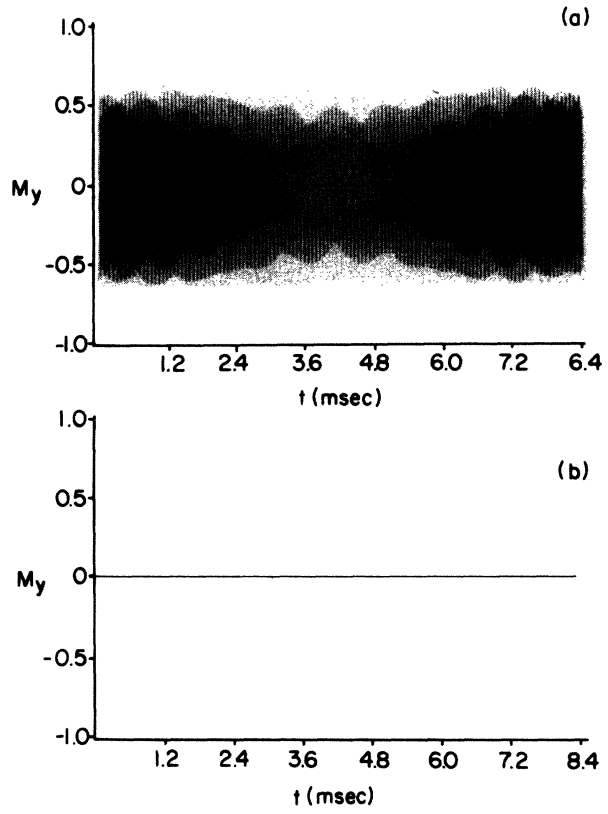

FIG. 21. Cancellation of rapid nonresonant oscillation of M_y with alternation of phase parameter β. (a) Irradiation as in Fig. 20(f); (b) with addition of second acquisition for which $\beta=\pi$.

resonances through $N=7$ are readily compared in Fig. 20, which presents the calculated resonant component of transverse magnetization induced by four fields having in each instance the same set of initial phases (only the intensities and spacing parameters are varied). In every case, the nutation axis is as predicted by Eqs. 43(a) and 43(b). From these panels the calculated t_π's can be compared with the theory for the seven-photon resonances. Thus for $k=1$, $l=6$, $t_\pi(\text{calc})=17$ ms, $t_\pi(\text{pred})=12$ ms; for $k=2$, $l=5$, $t_\pi(\text{calc})=10$ ms, $t_\pi(\text{pred})=7.5$ ms; for $k=3$, $l=4$, $t_\pi(\text{calc})=8.0$ ms, $t_\pi(\text{pred})=6.2$ ms. These times are not only in reasonable agreement with Eq. (42), but seem remarkably short for pulsed NMR resonances of seventh order. At the formal limit of the first-order theory ($\omega_0=\omega_i=\omega$) t_π's of ~ 10 ms are obtained for $\omega/2\pi \approx 10$ kHz.

A four-step phase cycle comparable to those of Table II was not identified for any seven-photon resonance or the $k=1$, $l=4$ five-photon resonance. Nevertheless, incrementing either α or β by π with successive acquisitions cancels the component of rapid oscillation orthogonal to the direction of resonant precession. The phase parameter alternated is that which corresponds to the field pair contributing an even number of photons [Eq. (37)]. Figure 21 illustrates the cancellation of the nonresonant ($\hat{\mathbf{y}}$) oscillation for the $k=3$, $l=4$ resonance ($\gamma=\pi/2$) with cycling of β.

IV. CONCLUSION

A theoretical analysis of the pulse four-field experiment has been presented which demonstrates the existence of a new class of multiphoton resonances in spins systems with $I=\frac{1}{2}$. For each resonance, there is a characteristic dependence of the effective multiphoton irradiation field on the amplitudes and initial phases of the rf components, and a number of mutually interfering transition pathways contribution to this effective field. Spiral motions typical of resonances induced by doubly-frequency irradiation are here readily suppressed. Extension of this work to spin $\frac{3}{2}$ and dipolar coupled spin systems is anticipated, with particular regard to selective off-resonance excitation of NMR transitions by manipulation of the rf field phases.

[1]H. Salwen, Phys. Rev. **99**, 1274 (1955).
[2]C. Besset, J. Horovitz, A. Messiah, and J. Winter, J. Phys. Radiat. **15**, 251 (1954).
[3]J. Winter, C.R. Acad. Sci. **241**, 375 (1955).
[4]J. Shirley, Ph.D. thesis, California Institute of Technology (1963).
[5]J. Shirley, Phys. Rev. **138B**, 979 (1965).
[6]J. V. Moloney and W. J. Meath, Mol. Phys. **31**, 1537 (1976).
[7]C. Cohen-Tannoudji, in *Cargese Lectures in Physics,* edited by M. Levy (Gordon and Breach, New York, 1968), Vol. II, p. 347.
[8]S. Wilking, Z. Phys. **173**, 490 (1963).
[9]T. Yabuzaki, Y. Murakami, and T. Ogawa, J. Phys. B **9**, 9 (1976).
[10]A. Autler and C. H. Townes, Phys. Rev. **100**, 703 (1955).
[11]J. Margerie and J. Brossel, C.R. Acad. Sci. **241**, 373 (1955).
[12]A. Abragam, *Principles of Nuclear Magnetism* (Oxford University, Oxford, 1961), Chap. II.
[13]W. A. Anderson, Phys. Rev. **102**, 151 (1956).
[14]J. R. Franz and C. P. Slichter, Phys. Rev. **148**, 287 (1966).
[15]P. Bucci, P. Cavalieri, and S. Santucci, J. Chem. Phys. **52**, 4041 (1970).
[16]P. Bucci, M. Martinelli, and S. Santucci, J. Chem. Phys. **53**, 4524 (1970).
[17]P. Bucci and S. Santucci, Phys. Rev. A **2**, 1105 (1970).
[18]Y. Zur, M. H. Levitt, and S. Vega, J. Chem. Phys. **78**, 5293 (1983).
[19]Y. Zur and S. Vega, J. Chem. Phys. **79**, 548 (1983).
[20]M. M. Maricq, Phys. Rev. B **25**, 6622 (1982).
[21]V. Mizrahi, Y. Prior, and S. Mukamel, Opt. Lett. **8**, 145 (1983).

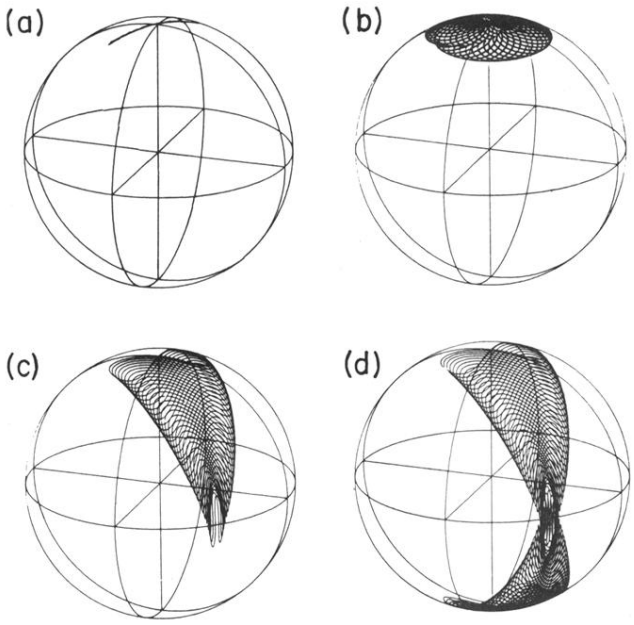

FIG. 11. Calculated motion of magnetization vector during multifrequency irradiation; $k=1$, $l=2$ (three-photon resonance). In each case $\alpha=\beta=0$, $\gamma=-\pi/4$. In this and all subsequent simulations, the phase parameter δ is fixed by $\delta=\gamma+\pi/2$ [Eq. (39′)]. (a) $\nu_1=\nu_4=0$, $\nu_2=\nu_3=4$ kHz, $t=3.21$ ms; (b) $\nu_3=\nu_4=0$, $\nu_1=\nu_2=4$ kHz, $t=3.21$ ms; (c) $\nu_1=\nu_2=\nu_3=\nu_4=4$ kHz, $t=1.61$ ms; (d) as in (c), $t=3.21$ ms.

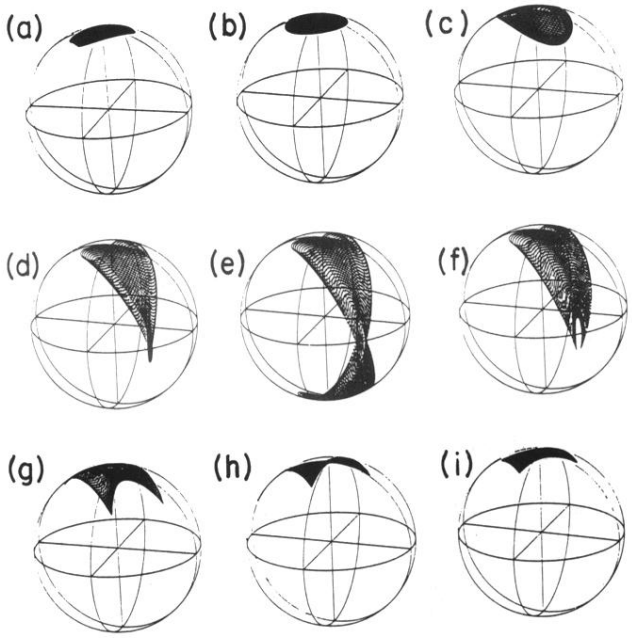

FIG. 12. Motion of magnetization near three-photon resonance: outer-field separation varied, inner-field separation constant at 40 kHz. For each plot $\alpha=\beta=0$, $\gamma=-\pi/4$, $\nu_j=4$ kHz for all j, $t=3.21$ ms. The outer-field separations are (a) 86 kHz, (b) 82 kHz, (c) 80.6 kHz, (d) 80.2 kHz, (e) 80 kHz, (f) 79.8 kHz, (g) 79.4 kHz, (h) 78 kHz, and (i) 74 kHz. Axes as in Fig. 8(a).

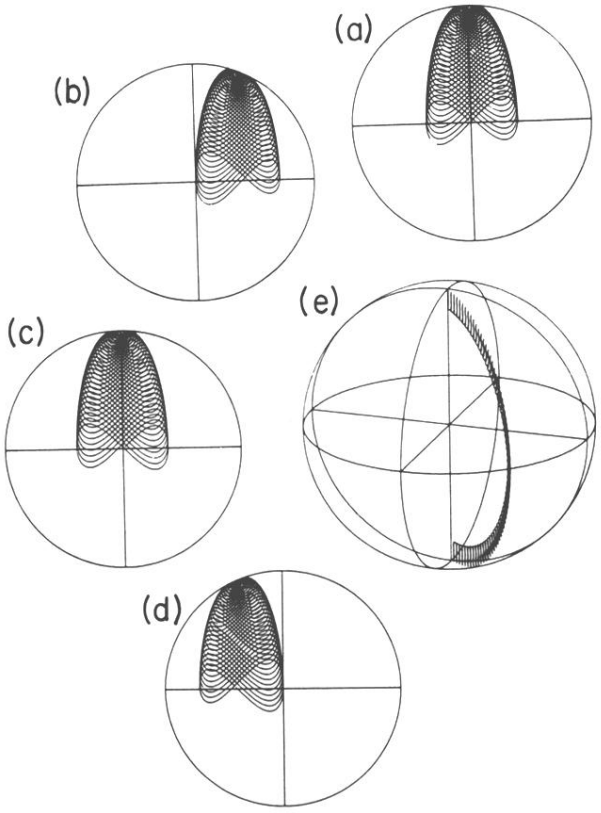

FIG. 14. Motion of spins at three-photon resonance. Irradiation parameters in kHz are as in Fig. 12(e). (a)–(d) phase $\gamma = 0°$; (e) phase $\gamma = -\pi/4$ for clarity. (a) $\alpha = 0$, $\beta = 0$; (b) $\alpha = \pi$, $\beta = \pi/2$; (c) $\alpha = 0$, $\beta = \pi$; (d) $\alpha = \pi$, $\beta = -\pi/2$; (e) average of (a)–(d).

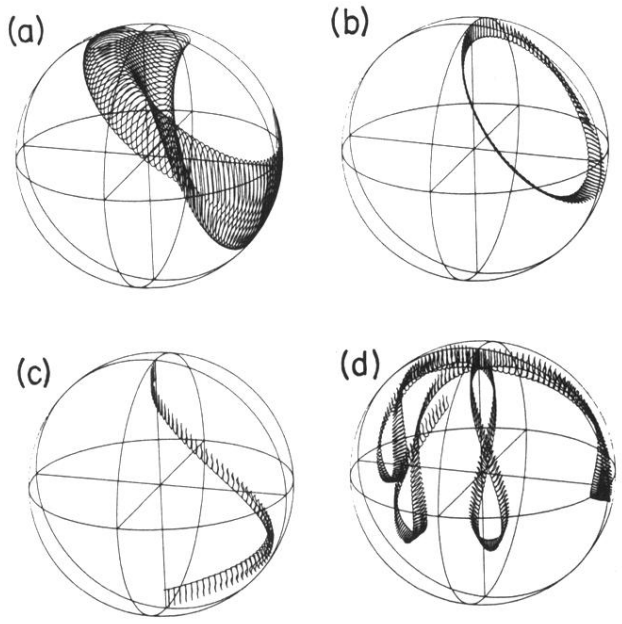

FIG. 16. Motion of magnetization for the three-photon ($k=1$, $l=2$) resonance. In each case $\omega/2\pi=20$ kHz, $\alpha=\beta=0$, $\gamma=-\pi/2$. (a) Field intensities not symmetric, zero offset; $\nu_1=\nu_2=3.8$ kHz, $\nu_3=\nu_4=4.2$ kHz, $t=3.2$ ms. (b) As in (a), with phase cycling, $t=6.4$ ms. (c) As in (a), with phase cycling, offset equal to 122 Hz. (d) All field intensities are 4 kHz, offset equal to 122 Hz, $t=20$ msec, with phase cycling.

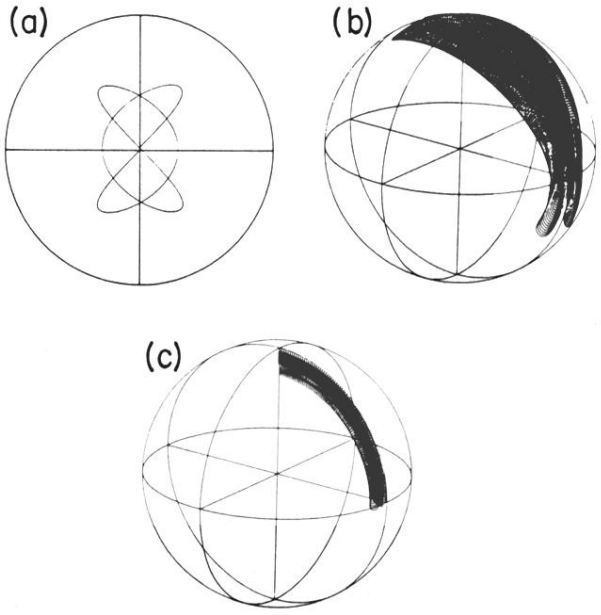

FIG. 18. Calculated motion of magnetization for the five-photon ($k=2$, $l=3$) resonance. All field strengths are 10 kHz, phases $\alpha=\beta=0$, $\gamma=\pi/2$. (a) $t=0.05$ ms, projection in xy plane; (b) $t=4.0$ ms; (c) $t=4.0$, with phase cycling (Table II).

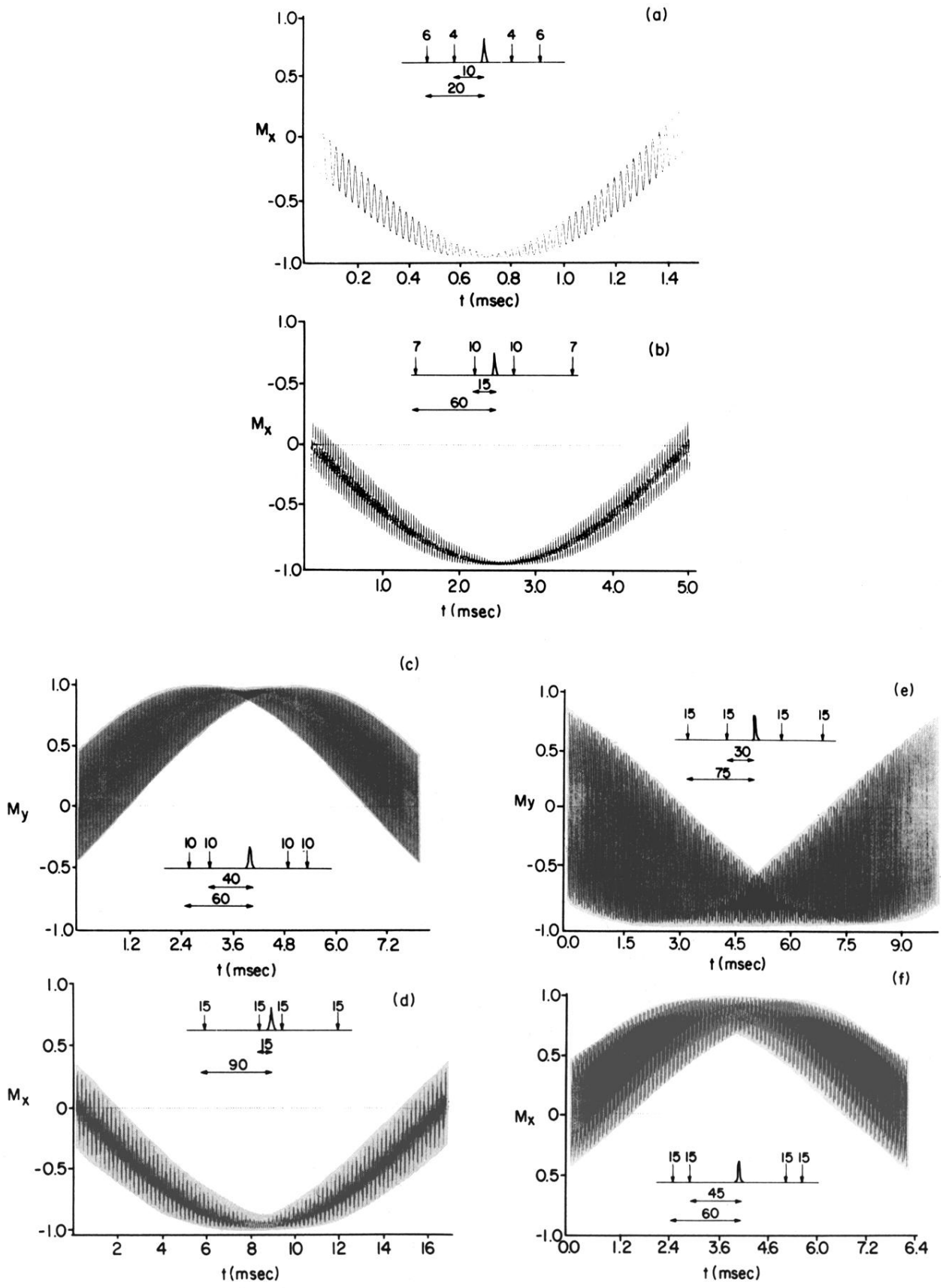

FIG. 20. Calculated resonant compound of the magnetization for multiphoton resonances from $N=3$ to 7. The field separations and intensities (in kHz) are indicated in the figure. In each case $\alpha=\beta=0$, $\gamma=\pi/2$. (a) Three photons, $k=1$, $l=2$; (b) five photons, $k=1$, $l=4$; (c) five photons, $k=2$, $l=3$; (d) seven photons, $k=1$, $l=6$; (e) seven photons, $k=2$, $l=5$; (f) seven photons, $k=3$, $l=4$.

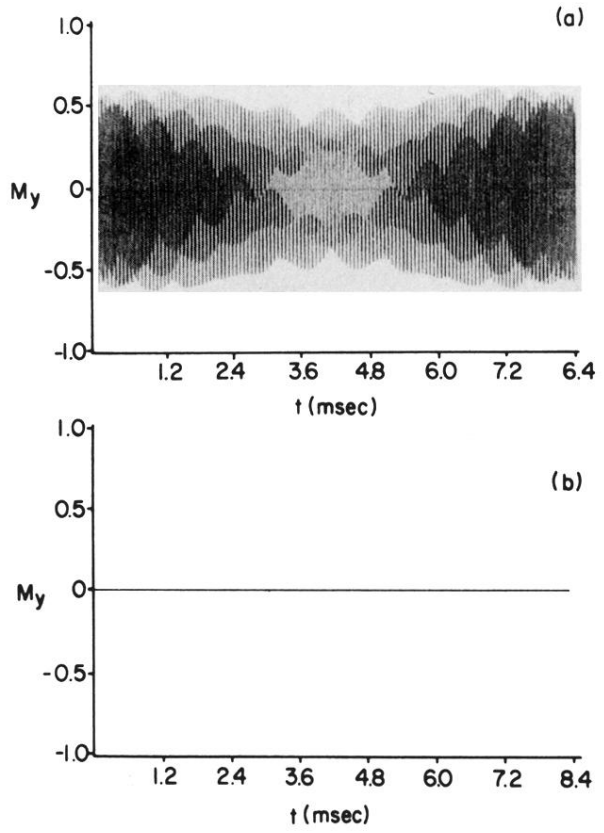

FIG. 21. Cancellation of rapid nonresonant oscillation of M_y with alternation of phase parameter β. (a) Irradiation as in Fig. 20(f); (b) with addition of second acquisition for which $\beta=\pi$.